



# Dynamic analysis of the response of Duffing-type oscillators subject to interacting parametric and external excitations

Mehrdad Aghamohammadi · Vladislav Sorokin · Brian Mace

Received: 30 January 2021 / Accepted: 6 October 2021 / Published online: 31 October 2021  
© The Author(s), under exclusive licence to Springer Nature B.V. 2021

**Abstract** Prediction of the response of nonlinear dynamical systems under interacting parametric and external excitations is important in designing systems such as sensors, amplifiers or energy harvesters, to achieve the desired performance. This paper concerns the nonlinear forced Mathieu equation, with linear damping and a 2:1 ratio between the parametric and external excitation frequencies. The Method of Varying Amplitudes (MVA) is employed to derive approximate analytical expressions for the response of the system. Both single-term and double-term solutions are developed: it is seen that, employing the double-term approximation, the MVA can accurately predict the response of the system over a wide range of frequencies and system parameters, showing a maximum of 0.2% deviation from numerical results obtained by direct integration of the equation of motion. This is in contrast with most of the available theoretical approaches such as the conventional Method of Multiple Scales, which can predict the response accurately only for a narrow range of system parameters and excitation frequencies. Furthermore, it

is seen that the response is bounded, and analytical expressions for the frequency and amplitude of the upper bound are developed: this is unlike other methods which predict unbounded response, unless nonlinear damping is considered. Analytical expressions for the response are developed, and results are verified with numerical results obtained from direct integration of the equation of motion. Numerical examples are presented, showing good agreement with results obtained by the MVA.

**Keywords** Nonlinear dynamical systems · Interacting parametric and external excitations · Bounded response · Nonlinear forced Mathieu equation · Method of varying amplitudes · Method of multiple scales

## 1 Introduction

In mechanical and electromechanical contexts, a system is referred to as parametrically excited (PE) when at least one of its parameters varies periodically with time. Altering the system orbits in the phase space, parametric excitation has been seen to enhance (i.e., to increase) the output response of the system. This kind of excitation has been observed in various physical systems such as marine risers [1], ships under parametric rolling induced by wave excitation [2, 3]

---

M. Aghamohammadi (✉) · V. Sorokin · B. Mace  
Department of Mechanical Engineering, University of  
Auckland, Auckland 1142, New Zealand  
e-mail: magh798@aucklanduni.ac.nz

V. Sorokin  
e-mail: v.sorokin@auckland.ac.nz

B. Mace  
e-mail: b.mace@auckland.ac.nz

and cable-supported structures [4, 5]. Parametric excitation has been exploited extensively in the literature in a wide range of applications from sensing [6–8], to energy harvesting [9–19] and response amplification [20–28].

Exploiting parametric excitation has shown the capability to enhance the performance of dynamical systems. It has been pointed out that the sensitivity of simple harmonic resonance-based mass sensors can be increased significantly when operated in the parametric resonance mode [8]. Energy harvesters subjected to parametric excitation exhibit better performance compared to externally excited ones. The operational bandwidth of these devices can be notably broadened by introducing some kind of nonlinearity into the system [13]. However, if not taken into account, parametric excitation might have disastrous effects on systems. Parametrically excited roll motion of a ship can cause a chaotic behavior which may capsize the ship if the system parameters are not adjusted accurately [2, 3]. Furthermore, periodic heave motion of marine risers may endanger the safe operation of these structures even with a small perturbation in the lateral direction [1]. Therefore, investigating the dynamic behavior of parametrically excited systems and the impact of the system parameters on their performance are of key significance. This can provide useful insights into how to exploit parametric excitation to enhance performance or prevent catastrophic effects on a system as a result of operating at frequencies close to parametric resonance frequencies.

Traditionally, perturbation methods have been used to study the dynamic behavior of PE systems [29–32]. These methods are based on assuming that the excitation is weak. Then, the response of the system is obtained by defining a small frequency detuning parameter around the principal parametric resonance, which is twice the natural frequency of the system, and solving the final autonomous system of equations [33]. They have proved to be able to accurately predict the response of the system for a frequency range around the principal parametric resonance. However, their accuracy is a function of the system parameters and the frequency detuning parameter. It has been pointed out that they cannot predict the response of the system correctly for arbitrary values of the system parameters and excitation frequencies considered [34]. In recent years, qualitative methods have been used to predict the response of parametrically excited systems,

particularly around bifurcation points [35]. However, the accuracy of these methods deteriorates as insufficient data are usually available for a frequency range close to the considered bifurcation frequency.

Correct estimation of the response of PE systems has a key role in evaluating their performance. Particularly, developing an analytical approach that can provide accurate predictions of the response of the system in frequency ranges away from the principal parametric resonance has attracted significant attention [34, 35]. This is the focus of this paper. Most of the available theoretical approaches fail to provide useful insight into the response of PE systems with a hardening Duffing-type nonlinearity for the whole frequency range considered [34]. Numerous studies on this subject area can be found in the literature which involves introducing nonlinear damping into the equation of motion or modifying the frequency detuning parameter in conventional perturbation techniques [36–43]. Nevertheless, the results are only accurate if the assumptions applied are satisfied, e.g., when the excitation frequency increases, the frequency detuning parameter cannot be assumed to be a small parameter any more, causing the accuracy of predictions to decrease. Furthermore, the question remains as how to develop accurate predictions, particularly a bounded response, without imposing restrictions on the frequency ranges and damping types.

It is known that conventional perturbation techniques can predict the response accurately for small system parameters and around the principal parametric resonance. However, their accuracy deteriorates as the excitation frequency increases, i.e., for systems with the Duffing type hardening nonlinearity and linear damping they predict an unbounded response [34]. It was proposed that nonlinear damping must be introduced into the governing equation of motion to enable perturbation methods to obtain a bounded response [39, 40]. Notably, although a bounded response can be achieved analytically this way, the response is highly dependent on the nonlinear damping coefficient and it implies the new challenge of determining the value of this coefficient. Also, it has been pointed out that the accuracy of the results will still be dependent on having small values for the system parameters [40]. This is due to the limitation of perturbation techniques in requiring the system parameters to be small and the excitation frequency

to be around the principal parametric resonance. For large upper bound responses away from the principal parametric resonance frequency, the Duffing nonlinear term is large and cannot be assumed to be small. Therefore, an approximation developed based on this assumption is not correct.

In contrast with the methods mentioned above, which require the system parameters to be small and the excitation frequencies to be around resonance, the method of varying amplitudes (MVA) has proved to be able to accurately predict the behavior of PE systems for the whole frequency range considered and has shown itself to be a useful technique for handling both linear and nonlinear problems [44–47]. In the present paper, we exploit parametric and external excitations simultaneously in order to increase the output response of PE systems. Employing the MVA, we show that the response is bounded, even in the presence of only linear damping, in contrast with prior observations that arise from perturbation (small parameter) analysis [32, 34, 48, 49].

The paper is focused on the analysis of the response of the nonlinear forced Mathieu equation without the commonly imposed restrictions on the frequency range considered or requiring nonlinear damping to be present in the equation of motion. The perfectly tuned case is studied, where the parametric excitation frequency is exactly twice the external excitation frequency. Employing the MVA, analytical expressions are developed for the output response of the system and bifurcation frequencies which are valid for the whole frequency range considered. The MVA results show that, for hardening type Duffing nonlinearity, the response of the system is bounded. This is in contrast with conclusions drawn from conventional perturbation methods, which predict an infinite growth of the response as the excitation frequency increases [21]. Explicit closed-form analytical expressions for the upper bound to the response of the system and the frequency at which it is attained are provided, which are of key importance for achieving optimal performance. Furthermore, the transition of the system response from pure parametrically excited to the case where external excitation dominates is studied, with the corresponding values for the critical external excitation amplitude being provided.

The governing equations describing a PE system with Duffing type (cubic) nonlinearity subject to interacting parametric and external excitations are

presented in Sect. 2. Employing the MVA, analytical expressions describing the steady state approximate response of the system are developed using both single-term and double-term approximations of the solution. Furthermore, to provide a useful insight into the system behavior, utilizing the single-term MVA approximation, closed-form analytical expressions for the upper bound to the response of the system and the frequency at which it is attained are found. The results are discussed and verified numerically by Direct Integration (DI) of the equation of motion in Sect. 3. In addition, results using the first- and second-order approximations of the response by the Method of Multiple Scales (MMS) are presented for comparison. Finally, conclusions are drawn in Sect. 4.

## 2 Mathematical model and MVA solutions

The response of a dynamical system with Duffing type nonlinearity under interacting parametric and external excitations is investigated. The parametric excitation frequency is tuned to be exactly twice the external excitation frequency. The proposed system can be modeled by the nonlinear forced Mathieu equation with linear damping

$$\ddot{u} + \beta\dot{u} + \omega_0^2(1 + P \cos(\Omega t))u + \eta u^3 = d \cos\left(\frac{1}{2}\Omega t + \varphi\right), \quad (1)$$

where  $u$  represents the displacement response of the system (e.g., the displacement of a pendulum hanging under gravity, whose support is subjected to a combined horizontal and vertical sinusoidal excitation),  $\dot{u}$  and  $\ddot{u}$  are the first and the second derivatives of  $u$  with respect to time, respectively, and  $\Omega$  represents the parametric excitation frequency. Furthermore,  $\beta$  is the damping ratio,  $\omega_0$  is the linear undamped natural frequency,  $P$  is the parametric excitation amplitude,  $d$  is the external excitation amplitude,  $t$  is time,  $\varphi$  is the phase angle between the parametric and external excitations, and  $\eta$  is the nonlinear coefficient. We note that in this paper we only consider the hardening case, where  $\eta > 0$ , as is more relevant for practical applications [6–28].

## 2.1 Steady-state approximate solution: single-term MVA approximation

To obtain an approximate solution to the response of the system modeled as (1), the MVA is used [44]. Employing the MVA,  $u(t)$  is considered as the sum

$$u(t) = \sum_{m=1}^n \left( C_m(t) \cos\left(\frac{1}{2}m\Omega t\right) + D_m(t) \sin\left(\frac{1}{2}m\Omega t\right) \right), \quad (2)$$

implying harmonics with time varying amplitudes  $C_m(t)$  and  $D_m(t)$ . The time dependency of the amplitudes allows the stability of the response to be investigated. Note that for the system considered here with cubic Duffing type nonlinearity, only odd values of  $m$  ( $m = 1, 3, \dots$ ) need to be considered in Eq. (2). Using the single-term MVA approximation ( $m = n = 1$ ), and omitting the index 1,  $u(t)$  is approximated as

$$u(t) = C(t) \cos\left(\frac{1}{2}m\Omega t\right) + D(t) \sin\left(\frac{1}{2}m\Omega t\right). \quad (3)$$

Substituting Eq. (3) into Eq. (1) and separating coefficients of  $\cos(\frac{1}{2}m\Omega t)$  and  $\sin(\frac{1}{2}m\Omega t)$  yield

$$\begin{aligned} \ddot{C} + \beta\dot{C} + \Omega\dot{D} + \frac{1}{2}\beta\Omega D \\ + \left( \omega_0^2 \left( 1 + \frac{1}{2}P \right) - \frac{1}{4}\Omega^2 \right) C + \frac{3}{4}\eta(C^2 + D^2)C \\ = d \cos(\varphi), \end{aligned} \quad (4)$$

$$\begin{aligned} \left( \ddot{D} - \Omega\dot{C} + \beta\dot{D} - \frac{1}{2}\beta\Omega C + \left( \omega_0^2 \left( 1 - \frac{1}{2}P \right) - \frac{1}{4}\Omega^2 \right) D \right) \sin\left(\frac{1}{2}\Omega t\right) \\ + \left( \frac{3}{4}\eta(C^2 + D^2)D + d \sin(\varphi) \right) \sin\left(\frac{1}{2}\Omega t\right) \\ = -\left( \frac{1}{2}P\omega_0^2 + \frac{1}{4}\eta(C^2 - 3D^2) \right) C \cos\left(\frac{3}{2}\Omega t\right) \\ - \left( \frac{1}{2}P\omega_0^2 + \frac{1}{4}\eta(3C^2 - D^2) \right) D \sin\left(\frac{3}{2}\Omega t\right). \end{aligned} \quad (5)$$

Assuming the terms  $\eta u^3$  and  $\omega_0^2 P u$  are small compared to the term  $\omega_0^2 u$ , one can neglect the higher-order harmonics on the right-hand side of Eq. (5), yielding

$$\begin{aligned} \ddot{D} - \Omega\dot{C} + \beta\dot{D} - \frac{1}{2}\beta\Omega C \\ + \left( \omega_0^2 \left( 1 - \frac{1}{2}P \right) - \frac{1}{4}\Omega^2 \right) D + \frac{3}{4}\eta(C^2 + D^2)D \\ + d \sin(\varphi) \\ = 0. \end{aligned} \quad (6)$$

Solving Eq. (4) and Eq. (6) for the steady state solution ( $\dot{C} = \dot{D} = \ddot{C} = \ddot{D} = 0$ ), the steady-state response of the system is obtained as

$$u(t) = C \cos\left(\frac{1}{2}\Omega t\right) + D \sin\left(\frac{1}{2}\Omega t\right). \quad (7)$$

To obtain the frequency response equation,  $u(t)$  in Eq. (3) can be rewritten as

$$u(t) = A(t) \cos\left(\frac{1}{2}\Omega t + \alpha(t)\right), \quad (8)$$

where  $A(t)$  is the amplitude and  $\alpha(t)$  is the phase, given by

$$A(t) = \sqrt{C(t)^2 + D(t)^2}, \quad \alpha(t) = \tan^{-1}\left(\frac{-D(t)}{C(t)}\right). \quad (9)$$

For  $A$  and  $\alpha$ , we then obtain

$$\begin{aligned} \ddot{A} + \beta\dot{A} + \left( \omega_0^2 \left( 1 + \frac{1}{2}P \cos(2\alpha) \right) - \frac{1}{4}\Omega^2 \right) A + \frac{3}{4}\eta A^3 \\ = d \cos(\varphi - \alpha), \end{aligned} \quad (10)$$

$$-\Omega\dot{A} - \frac{1}{2}\beta\Omega A + \frac{1}{2}\omega_0^2 P A \sin(2\alpha) = -d \sin(\varphi - \alpha). \quad (11)$$

Consequently, solving Eqs. (10) and (11) for the steady-state solution, the frequency response equation is obtained as

$$\begin{aligned} 9\eta^2 A^6 - 6\eta(\Omega^2 - 4\omega_0^2)A^4 - 24d\eta \cos(\varphi - \alpha)A^3 \\ + (\Omega^4 + 4\Omega^2(\beta^2 - 2\omega_0^2) + 4\omega_0^4(4 - P^2))A^2 \\ + 8d((\Omega^2 - 4\omega_0^2) \cos(\varphi - \alpha) - 2\beta\Omega \sin(\varphi - \alpha))A \\ + 16d^2 \\ = 0. \end{aligned} \quad (12)$$

Equation (12) yields 6 solutions for  $A$ , with only real, positive solutions being physically meaningful

(There are in fact a maximum of 5 such solutions [42]). As  $\Omega^2 \rightarrow \infty$  the response is bounded, with there being only one real solution to (12). This can be seen by retaining only the leading terms in  $\Omega^2$  and  $A^2$  so that Eq. (12) reduces to

$$9\eta^2 A^4 - 6\eta(\Omega^2 - 4\omega_0^2)A^2 + (\Omega^4 + 4\Omega^2(\beta^2 - 2\omega_0^2)) \approx 0. \tag{13}$$

The radicand when solving this quadratic in  $A^2$  and assuming  $\Omega^2 \rightarrow \infty$  reduces to  $-144\eta^2\Omega^2\beta^2$ : the corresponding solutions for  $\Omega^2 \rightarrow \infty$  are therefore complex and not physically meaningful. This is in contrast with the single-term solution using MMS which predicts an unbounded response with  $\Omega^2 \rightarrow \infty$  (see Sect. 3).

For example, Fig. 1 shows the frequency response as a function of the frequency ratio  $\Omega/\omega_0$  for the set of system parameters  $\beta = 0.1$ ,  $\eta = 0.05$ ,  $\omega_0 = 1$ ,  $P = 0.3$ ,  $d = 0.1$ , and  $\varphi = -\pi/4$ . It is divided into 5 separate frequency regions bounded by the frequencies  $\Omega_1 = 1.97$ ,  $\Omega_2 = 2.17$ ,  $\Omega_3 = 2.88$  and  $\Omega_4 = 3.10$ . The response of the system is bounded, in contrast with the single-term solution using MMS: the upper bound amplitude is  $A = 19.38$  and is attained at the

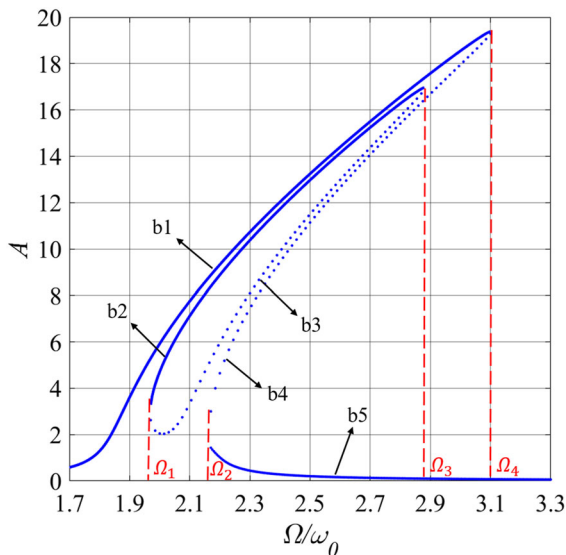


**Fig. 1**  $A$  as a function of  $\Omega/\omega_0$  obtained from the single-term approximation of the MVA using the frequency response Eq. (12). Solid lines denote the stable solutions, and dotted lines denote the unstable solutions ( $\beta = 0.1$ ,  $\eta = 0.005$ ,  $\omega_0 = 1$ ,  $P = 0.3$ ,  $\varphi = -\pi/4$ ,  $d = 0.1$ )

frequency  $\Omega_4$ . We note that the upper bound frequency  $\Omega_4$  has not been determined or discussed previously for the case of linear damping, cf., e.g., [21, 48].

### 2.2 Stability analysis

Unlike the conventional method of harmonic balance, where the amplitudes are constants and the stability of the response cannot be investigated, the MVA allows the stability of the response to be analyzed directly. To this end, the Jacobian matrix is considered [33]. From Eqs. (4) and (6), one can define

$$x_1 = C, \quad x_2 = \dot{C}, \quad x_3 = D, \quad x_4 = \dot{D}, \tag{14}$$

$$\begin{aligned} \dot{x}_2 = & - \left( \omega_0^2 \left( 1 + \frac{1}{2}P \right) - \frac{1}{4}\Omega^2 \right) x_1 - \beta x_2 - \frac{1}{2}\beta\Omega x_3 \\ & - \Omega x_4 - \frac{3}{4}\eta x_1 (x_1^2 + x_3^2) + d \cos(\varphi), \end{aligned} \tag{15}$$

$$\begin{aligned} \dot{x}_4 = & \frac{1}{2}\beta\Omega x_1 + \Omega x_2 - \left( \omega_0^2 \left( 1 - \frac{1}{2}P \right) - \frac{1}{4}\Omega^2 \right) x_3 \\ & - \beta x_4 - \frac{3}{4}\eta x_3 (x_1^2 + x_3^2) - d \sin(\varphi). \end{aligned} \tag{16}$$

The Jacobian matrix  $J$  is then defined as the  $4 \times 4$  matrix whose  $(i, j)$ th element is  $J_{ij} = \partial \dot{x}_i / \partial x_j$ . Consequently, the trace  $tr(J)$  and the determinant  $\Delta(J)$  of the Jacobian matrix are

$$tr(J) = -2\beta, \tag{17}$$

$$\begin{aligned} \Delta(J) = & \frac{1}{16}(\Omega^2 - 4\omega_0^2)^2 + \frac{1}{4}(\beta^2\Omega^2 - P^2\omega_0^4) \\ & - \frac{3}{4}\eta(\Omega^2 - 4\omega_0^2)(x_1^2 + x_3^2) \\ & + \frac{27}{16}\eta^2(x_1^2 + x_3^2)^2 + \frac{3}{4}\eta P\omega_0^2(x_3^2 - x_1^2). \end{aligned} \tag{18}$$

We note that hardening type nonlinearity is considered in this paper ( $\eta > 0$ ). For  $\beta > 0$ ,  $tr(J)$  is negative. Therefore, the response of the system is stable only if  $\Delta(J) > 0$  [33]. Consequently, branches b1, b2 and b5 in Fig. 1 are stable and branches b3 and b4 are unstable.

### 2.3 Steady-state approximate solution: double-term MVA approximation

To obtain more accurate analytical results, we take into account higher harmonics in the MVA, cf. also [34]. Employing the double-term approximation of the MVA, the response of the system is approximated using (2) for  $m = 1, 3$  as

$$u(t) = C_1(t) \cos\left(\frac{1}{2}\Omega t\right) + D_1(t) \sin\left(\frac{1}{2}\Omega t\right) + C_3(t) \cos\left(\frac{3}{2}\Omega t\right) + D_3(t) \sin\left(\frac{3}{2}\Omega t\right). \quad (19)$$

Substituting Eq. (19) into Eq. (1), and after some simplifications, the following system of equations is obtained:

$$\begin{aligned} \ddot{C}_1 + \beta\dot{C}_1 + \Omega\dot{D}_1 + \left(\omega_0^2\left(1 + \frac{1}{2}P\right) - \frac{1}{4}\Omega^2\right)C_1 \\ + \frac{1}{2}\beta\Omega D_1 + \frac{1}{2}\omega_0^2 P C_3 \\ + \frac{3}{4}\eta(C_1^3 + C_1(D_1^2 + 2D_1D_3 + 2C_3^2 + 2D_3^2) \\ + C_3(C_1^2 - D_1^2)) = d \cos(\varphi), \end{aligned} \quad (20)$$

$$\begin{aligned} \ddot{D}_1 - \Omega\dot{C}_1 + \beta\dot{D}_1 - \frac{1}{2}\beta\Omega C_1 \\ + \left(\omega_0^2\left(1 - \frac{1}{2}P\right) - \frac{1}{4}\Omega^2\right)D_1 + \frac{1}{2}\omega_0^2 P D_3 \\ + \frac{3}{4}\eta(D_1^3 + D_1(C_1^2 - 2C_1C_3 + 2C_3^2 + 2D_3^2) \\ + D_3(C_1^2 - D_1^2)) = -d \sin(\varphi), \end{aligned} \quad (21)$$

$$\begin{aligned} \ddot{C}_3 + \beta\dot{C}_3 + 3\Omega\dot{D}_3 + \frac{1}{2}\omega_0^2 P C_1 + \left(\omega_0^2 - \frac{9}{4}\Omega^2\right)C_3 \\ + \frac{3}{2}\Omega\beta D_3 + \frac{1}{4}\eta(C_1^3 + 3C_3^3 - 3C_1D_1^2 \\ + 3C_3(2C_1^2 + 2D_1^2 + D_3^2)) = 0, \end{aligned} \quad (22)$$

$$\begin{aligned} \ddot{D}_3 + \beta\dot{D}_3 - 3\Omega\dot{C}_3 + \frac{1}{2}\omega_0^2 P D_1 + \left(\omega_0^2 - \frac{9}{4}\Omega^2\right)D_3 \\ - \frac{3}{2}\Omega\beta C_3 + \frac{1}{4}\eta(-D_1^3 + 3C_1^3(D_1 + 2D_3) \\ + 3D_3(2D_1^2 + C_3^2 + D_3^2)) = 0. \end{aligned} \quad (23)$$

Consequently, the steady-state solution can be determined by setting all time derivatives in Eqs. (20) to (23) to zero and solving the resulting system of equations.

The analytical results of the single-term and double-term approximations of the MVA for a system under interacting parametric and external excitations are shown in Fig. 2 for comparison. The system parameters considered are  $\beta = 0.15$ ,  $\eta = 0.01$ ,  $\omega_0 = 1$ ,  $P = 0.5$ ,  $\varphi = -\pi/4$ , and  $d = 0.2$ . Results are compared with those obtained by direct numerical integration (DI) of the equation of motion (1). The Runge–Kutta method was applied to obtain the numerical results using a variable time step for each frequency (ode45 in MATLAB). The steady-state response found from DI converges to one of the stable solutions, which solution depends on the chosen initial conditions. While the single-term MVA results are in good qualitative agreement with DI results, the accuracy around the upper bound response is moderate. However, applying the double-term approximation of the MVA, the difference between the upper bound amplitude obtained analytically and that obtained numerically ( $A = 17.973$  at  $\Omega = 3.650$ ) is reduced significantly from 7.83% ( $A = 16.565$  at  $\Omega = 3.490$  in the single-term approximation) to 0.1% ( $A = 17.955$  at  $\Omega = 3.650$  in the double-term approximation).

### 2.4 Closed-form expressions for the upper bound of the system response from the MVA

Accurate prediction of the dynamic response of parametrically excited systems plays an important role in evaluating their performance in practical applications such as sensing, energy harvesting and response amplification. As shown in Sect. 2.3, the double-term approximation of the MVA can predict the response very accurately. While the single-term MVA approximation is less accurate, it can be used to develop closed-form analytical expressions which describe the main characteristics of the response. To

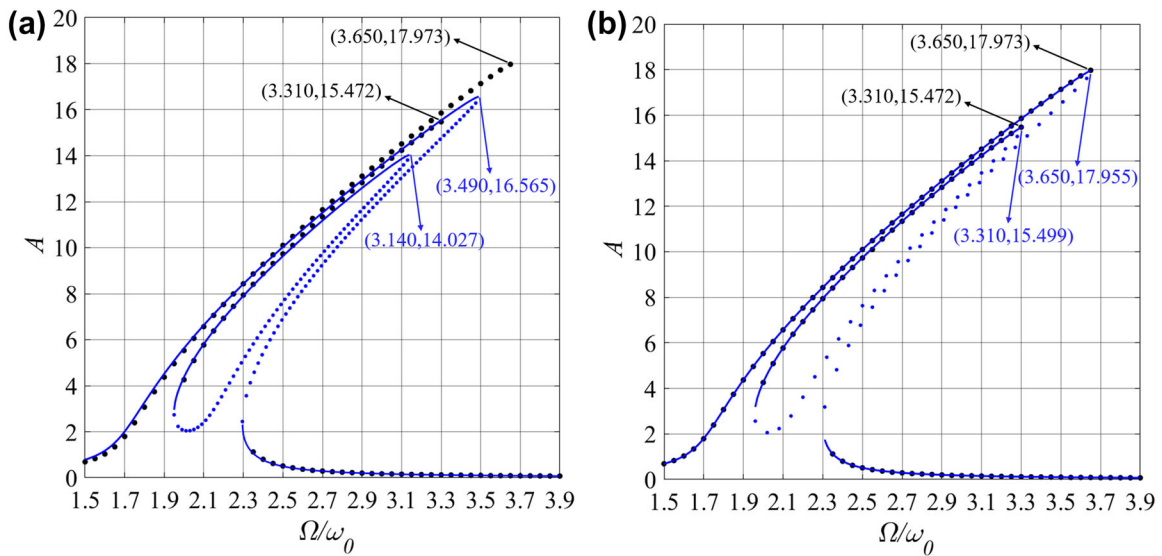


**Fig. 2** Response amplitude  $A$  as a function of frequency ratio  $\Omega/\omega_0$ , comparing the numerical results obtained by DI (black dots) with analytical results obtained by the MVA (blue color) applying **a** the single-term approximation using Eq. (12) and **b** the double-term approximation using Eqs. (19) to (23), for the

system under interacting parametric and external excitations. The solid lines and discrete data points represent the stable and unstable analytical results, respectively ( $\beta = 0.15$ ,  $\eta = 0.01$ ,  $\omega_0 = 1$ ,  $P = 0.5$ ,  $\varphi = -\pi/4$ ,  $d = 0.2$ )

investigate in detail the performance of the system under interacting external excitation using the single-term approximation of the MVA, in this section we analyze the response of the system by comparing it with the response of the equivalent parametrically excited system with no external excitation. For the equivalent system under pure parametric excitation ( $d = 0$ ), the frequency response Eq. (12) becomes

$$A_0^2(9\eta^2A_0^4 - 6\eta(\Omega^2 - 4\omega_0^2)A_0^2 + \Omega^4 + 4\Omega^2(\beta^2 - 2\omega_0^2) + 4\omega_0^4(4 - P^2)) = 0, \tag{24}$$

where  $A_0$  represents the amplitude response of the system under pure parametric excitation. Consequently, solving Eq. (24) for the nontrivial solution and considering Eq. (9),  $A_0$  and the phase  $\alpha_0$  for this system are obtained as

$$A_0 = \sqrt{\frac{1}{3\eta} \left( \Omega^2 - 4\omega_0^2 \pm 2\sqrt{(\omega_0^2 P)^2 - (\beta\Omega)^2} \right)}, \tag{25}$$

$$\sin(2\alpha_0) = \frac{\beta\Omega}{\omega_0^2 P},$$

where the positive sign represents the stable nontrivial response existing above the frequency  $\Omega_{c1}$  and the negative sign represents the unstable nontrivial

response existing above the frequency  $\Omega_{c2}$  (see Fig. 3), where  $\Omega_{c1}$  and  $\Omega_{c2}$  are

$$\Omega_{c1,2} = \sqrt{4\omega_0^2 - 2\beta^2 \mp 2\sqrt{\beta^2(\beta^2 - 4\omega_0^2) + (P\omega_0^2)^2}}. \tag{26}$$

The response of the system has an upper bound  $A_{u0}$  which is attained at the frequency  $\Omega_{u0}$ , where [34]

$$A_{u0} = \omega_0 \sqrt{\frac{(\omega_0 P)^2 - (2\beta)^2}{3\eta\beta^2}}, \quad \Omega_{u0} = \frac{\omega_0^2 P}{\beta}. \tag{27}$$

The amplitude response  $A_0$  of the system under pure parametric excitation, obtained from the single-term MVA approximation, is shown as a function of the frequency ratio in Fig. 3. For the set of system parameters considered,  $\Omega_{c1} = 1.88$ ,  $\Omega_{c2} = 2.10$ ,  $A_{u0} = 18.26$ , and  $\Omega_{u0} = 3.00$ .

Now consider the case where the system is under interacting parametric and external excitations. We introduce a small positive parameter  $\varepsilon \ll 1$ . Considering a small external excitation of amplitude  $d = \varepsilon d_1$  in Eq. (1),  $A$  and  $\alpha$  are written as the power series

$$A = A_0 + \varepsilon A_1 + \dots, \quad \alpha = \alpha_0 + \varepsilon \alpha_1 + \dots \tag{28}$$

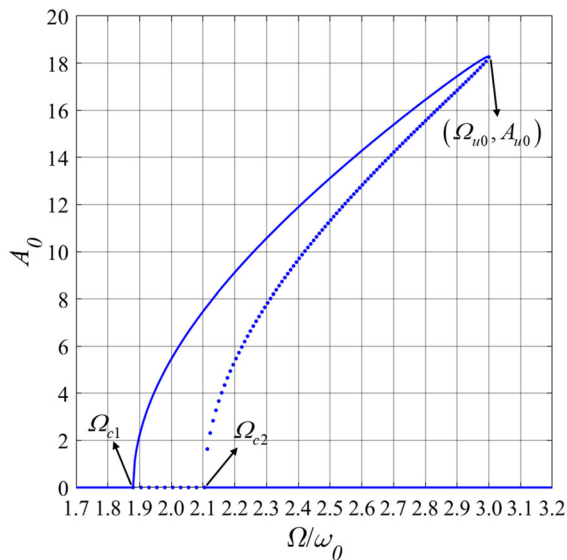


**Fig. 3** Response amplitude  $A_0$  as a function of  $\Omega/\omega_0$  for a dynamical system under pure parametric excitation with no external excitation obtained from the single-term approximation of the MVA. Solid lines denote the stable solutions, and dotted lines denote the unstable solutions ( $\beta = 0.1, \eta = 0.005, \omega_0 = 1, P = 0.3$ )

Consequently, substituting Eq. (28) into Eqs. (10) and (11) and separating the coefficients of the same power of  $\varepsilon$ , the steady-state solution can be obtained. Collecting the coefficients of order  $\varepsilon^0$  leads to Eq. (25) again, and collecting coefficients of order  $\varepsilon$  yields

$$\begin{aligned}
 & -\omega_0^2 P \alpha_1 \sin(2\alpha_0) A_0 \\
 & + \left( \omega_0^2 \left( 1 + \frac{1}{2} P \cos(2\alpha_0) \right) - \frac{1}{4} \Omega^2 + \frac{9}{4} \eta A_0^2 \right) A_1 \\
 & = d_1 \cos(\varphi - \alpha_0),
 \end{aligned} \tag{29}$$

$$\begin{aligned}
 & \omega_0^2 P \alpha_1 \cos(2\alpha_0) A_0 + \frac{1}{2} (\omega_0^2 P \sin(2\alpha_0) - \beta \Omega) A_1 \\
 & = -d_1 \sin(\varphi - \alpha_0).
 \end{aligned} \tag{30}$$

Solving Eqs. (29) and (30), it can be seen that when a small external disturbance is added, the stable non-trivial branch of the system response with no external excitation will split into a pair of stable branches (see Fig. 4). This is due to degeneracy of the solutions. When  $d = 0$ , for parametric excitation of period  $2\pi/\Omega$  the solutions come as a pair  $u(t)$  and  $-u(t)$ , both of period  $4\pi/\Omega$ . When  $d > 0$ , the two solutions differ.

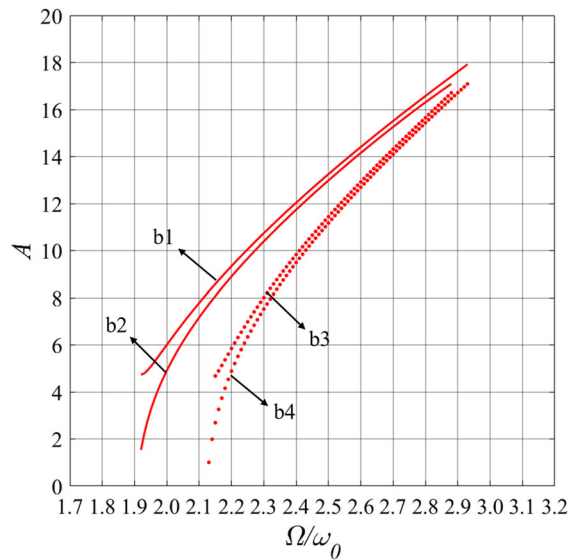


**Fig. 4** Response amplitude  $A$  as a function of  $\Omega/\omega_0$  obtained from implementing the small parameter expansion of the frequency response Eq. (12) using Eqs. (33) and (34) for a frequency range away from  $\Omega_{u0}$  ( $\beta = 0.1, \eta = 0.005, \omega_0 = 1, P = 0.3, \varphi = -\pi/4$ , and  $d = 0.1$ )

For the stable branches b1 and b2, the phases are given by

$$\begin{aligned}
 \alpha_{b1} = & \frac{\pi}{2} - \frac{1}{2} \sin^{-1} \left( \frac{\beta \Omega}{\omega_0^2 P} \right) \\
 & + \frac{\sqrt{3\eta} d \cos \left( \varphi + \frac{1}{2} \sin^{-1} \left( \frac{\beta \Omega}{\omega_0^2 P} \right) \right)}{\sqrt{(\omega_0^2 P)^2 - (\beta \Omega)^2} \sqrt{\Omega^2 - 4\omega_0^2 + 2\sqrt{(\omega_0^2 P)^2 - (\beta \Omega)^2}}},
 \end{aligned} \tag{31}$$

$$\begin{aligned}
 \alpha_{b2} = & \frac{3\pi}{2} - \frac{1}{2} \sin^{-1} \left( \frac{\beta \Omega}{\omega_0^2 P} \right) \\
 & - \frac{\sqrt{3\eta} d \cos \left( \varphi + \frac{1}{2} \sin^{-1} \left( \frac{\beta \Omega}{\omega_0^2 P} \right) \right)}{\sqrt{(\omega_0^2 P)^2 - (\beta \Omega)^2} \sqrt{\Omega^2 - 4\omega_0^2 + 2\sqrt{(\omega_0^2 P)^2 - (\beta \Omega)^2}}},
 \end{aligned} \tag{32}$$

respectively. Also, the amplitude responses for branches b1 ( $A_{b1}$ ) and b2 ( $A_{b2}$ ) are

$$\begin{aligned}
 A_{b1,2} = & \sqrt{\frac{1}{3\eta} \left( \Omega^2 - 4\omega_0^2 + 2\sqrt{(\omega_0^2 P)^2 - (\beta \Omega)^2} \right)} \\
 & \mp \frac{2d \left( -\beta \Omega \cos \left( \varphi + \frac{1}{2} \sin^{-1} \left( \frac{\beta \Omega}{\omega_0^2 P} \right) \right) + \sqrt{(\omega_0^2 P)^2 - (\beta \Omega)^2} \sin \left( \varphi + \frac{1}{2} \sin^{-1} \left( \frac{\beta \Omega}{\omega_0^2 P} \right) \right) \right)}{\sqrt{(\omega_0^2 P)^2 - (\beta \Omega)^2} \left( \Omega^2 - 4\omega_0^2 + 2\sqrt{(\omega_0^2 P)^2 - (\beta \Omega)^2} \right)}.
 \end{aligned} \tag{33}$$



Similarly, as illustrated in Fig. 4, the unstable response branch of the corresponding system under pure parametric excitation depicted in Fig. 3 splits into two unstable branches b3 and b4 as a result of the external excitation. For these branches, the amplitude responses are obtained as

$$A_{b3,4} = \sqrt{\frac{1}{3\eta} \left( \Omega^2 - 4\omega_0^2 - 2\sqrt{(\omega_0^2 P)^2 - (\beta\Omega)^2} \right) \pm \frac{2d \left( -\beta\Omega \sin \left( \varphi - \frac{1}{2} \sin^{-1} \left( \frac{\beta\Omega}{\omega_0^2 P} \right) \right) + \sqrt{(\omega_0^2 P)^2 - (\beta\Omega)^2} \cos \left( \varphi + \frac{1}{2} \sin^{-1} \left( \frac{\beta\Omega}{\omega_0^2 P} \right) \right) \right)}{\sqrt{(\omega_0^2 P)^2 - (\beta\Omega)^2} \left( \Omega^2 - 4\omega_0^2 - 2\sqrt{(\omega_0^2 P)^2 - (\beta\Omega)^2} \right)}} \quad (34)$$

Furthermore, for these two branches

$$\alpha_{b3} = \frac{1}{2} \sin^{-1} \left( \frac{\beta\Omega}{\omega_0^2 P} \right) - \frac{\sqrt{3\eta d} \sin \left( \varphi + \frac{1}{2} \sin^{-1} \left( \frac{\beta\Omega}{\omega_0^2 P} \right) \right)}{\sqrt{(\omega_0^2 P)^2 - (\beta\Omega)^2} \sqrt{\Omega^2 - 4\omega_0^2 - 2\sqrt{(\omega_0^2 P)^2 - (\beta\Omega)^2}}}, \quad (35)$$

$$\alpha_{b4} = \pi + \frac{1}{2} \sin^{-1} \left( \frac{\beta\Omega}{\omega_0^2 P} \right) + \frac{\sqrt{3\eta d} \sin \left( \varphi + \frac{1}{2} \sin^{-1} \left( \frac{\beta\Omega}{\omega_0^2 P} \right) \right)}{\sqrt{(\omega_0^2 P)^2 - (\beta\Omega)^2} \sqrt{\Omega^2 - 4\omega_0^2 + 2\sqrt{(\omega_0^2 P)^2 - (\beta\Omega)^2}}}, \quad (36)$$

respectively.

The expansion (28) can accurately predict the behavior of the system except around the three critical frequencies  $\Omega_{c1}$ ,  $\Omega_{c2}$  and  $\Omega_{u0}$ , where it predicts an infinite response. To investigate the response of the system in the frequency range around the upper bound,  $\Omega_{u0}$ , we consider a small deviation from this frequency. Then,  $\alpha$  and  $A$  are obtained as

$$\alpha = \alpha_0 \pm \frac{\sqrt{-A_{u0}\beta(\Omega - \Omega_{u0}) - 2d \sin(\alpha_0 - \varphi)}}{\omega_0 \sqrt{2PA_{u0}}}, \quad (37)$$

$$A = A_{u0} + (\alpha - \alpha_0)A_{\varepsilon1} + A_{\varepsilon2}, \quad (38)$$

where  $\Omega_{u0}$  and  $A_{u0}$  can be obtained from Eq. (27) and values of  $\alpha_0$  are discussed below. Furthermore,  $A_{\varepsilon1}$  and  $A_{\varepsilon2}$  are defined as

$$A_{\varepsilon1} = \frac{4P\beta^2\omega_0^2 A_{u0}}{9\eta\beta^2 A_{u0}^2 + 4\beta^2\omega_0^2 - P^2\omega_0^4}, \quad (39)$$

$$A_{\varepsilon2} = \beta \left( (4P\beta\omega_0^2 A_{\varepsilon1} - 9\eta\beta A_{u0} A_{\varepsilon1}^2) (\alpha - \alpha_0)^2 + 2A_{u0} P \omega_0^2 (\Omega - \Omega_{u0}) + 4d\beta \cos(\alpha_0 - \varphi) \right) / (9\eta\beta^2 A_{u0}^2 + 4\beta^2\omega_0^2 - P^2\omega_0^4). \quad (40)$$

The positive sign in Eq. (37) corresponds to the branches b1 and b2 around  $\Omega_{u0}$ , and the negative sign corresponds to the branches b3 and b4. For b1 and b4,  $\alpha_0 = 5\pi/4$ , and for b2 and b3,  $\alpha_0 = \pi/4$ . The effects of applying a small external excitation to the system under pure parametric excitation for frequencies around  $\Omega_{u0}$  are depicted in Fig. 5, along with the results for frequencies away from  $\Omega_{u0}$  obtained from the first expansion (33), (34). As indicated, two critical frequencies appear as a result of adding a small external excitation amplitude:  $\Omega_{u1}$  is the frequency corresponding to the upper bound of branches b2 and b3, while  $\Omega_{u2}$  is the frequency at which the upper bound to the response of the system occurs, when branches b1 and b4 collide. The amplitude responses related to these critical frequencies are  $A_{u1}$  and  $A_{u2}$ ,

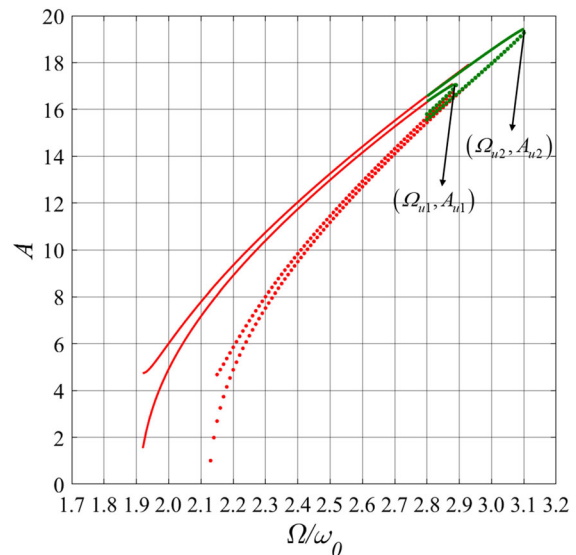


**Fig. 5** Response amplitude  $A$  as a function of  $\Omega/\omega_0$  obtained from the expansion for a frequency range away from  $\Omega_{u0}$  using Eqs. (33) and (34) (red color) and from the expansion for a frequency range around  $\Omega_{u0}$  using Eqs. (37) to (40) (green color). Solid lines represent the stable responses, and discrete points represent the unstable responses ( $\beta = 0.1$ ,  $\eta = 0.005$ ,  $\omega_0 = 1$ ,  $P = 0.3$ ,  $\varphi = -\pi/4$ ,  $d = 0.1$ )

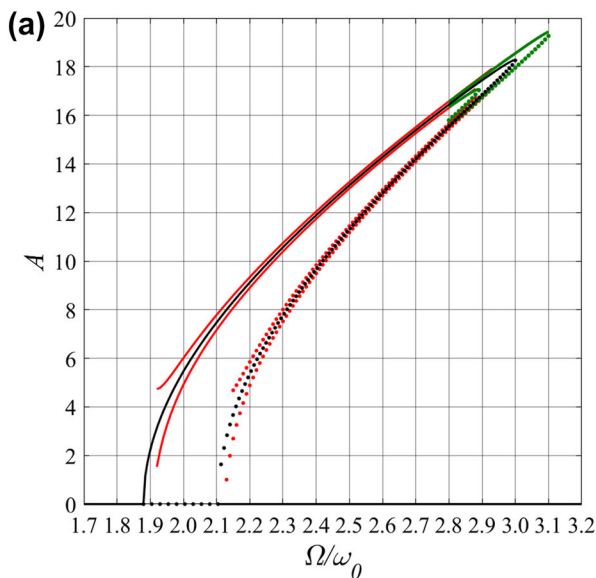


**Fig. 6** Response amplitude  $A$  as a function of  $\Omega/\omega_0$  obtained from the expansion for a frequency range away from  $\Omega_{u0}$  using Eqs. (33) and (34) (red color) and from the expansion for a frequency range around  $\Omega_{u0}$  using Eqs. (37) to (40) (green color) with: **a** the results corresponding to the system under pure parametric excitation with no external excitation ( $d = 0$ , black

respectively. Consequently, taking Eq. (26) into account, and using Eqs. (37) to (40),  $\Omega_{u1}$ ,  $\Omega_{u2}$ ,  $A_{u1}$  and  $A_{u2}$  are obtained as

$$\Omega_{u1,2} = \frac{\omega_0^2 P}{\beta} \mp \frac{2\sqrt{3}\eta d \cos(\frac{\pi}{4} + \varphi)}{\sqrt{(\omega_0^2 P)^2 - (2\beta\omega_0)^2}}, \tag{41}$$

$$A_{u1,2} = A_{u0} \mp \frac{2A_{u0}P\omega_0^2(\Omega_{u1,2} - \Omega_{u0})^2 - 4d\beta \cos(\frac{\pi}{4} - \varphi)}{9\eta\beta^2 A_{u0}^2 + 4\beta^2\omega_0^2 - P^2\omega_0^4}. \tag{42}$$

For the set of system parameters considered in Fig. 5,  $\Omega_{u1} = 2.89$ ,  $A_{u1} = 16.94$ ,  $\Omega_{u2} = 3.11$  and  $A_{u2} = 19.57$  while  $\Omega_{u0} = 3.00$  and  $A_{u0} = 18.26$ .

The responses of the system under pure parametric excitation and the PE system with a small external excitation added are shown in Fig. 6a for comparison. The system parameters considered are  $\beta = 0.1$ ,  $\eta = 0.005$ ,  $\omega_0 = 1$ ,  $P = 0.3$ ,  $\varphi = -\pi/4$  and  $d = 0.1$ . To illustrate the accuracy of the small parameter expansions, Fig. 6b shows the responses obtained by these expansions (red and green lines) and the direct implementation of Eq. (12) (blue lines). As can be

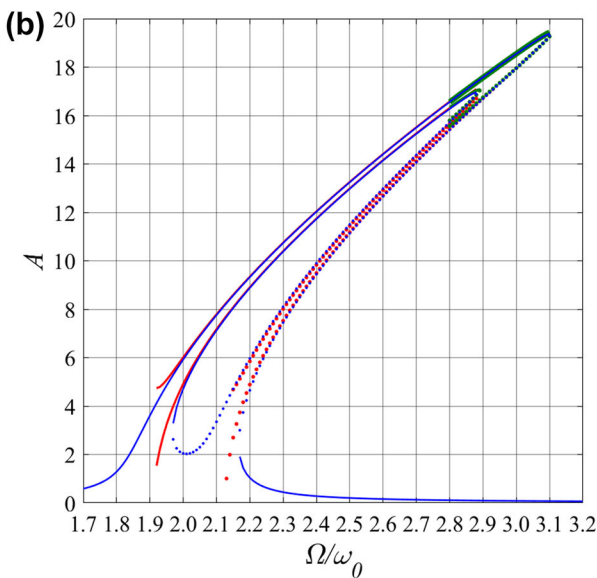


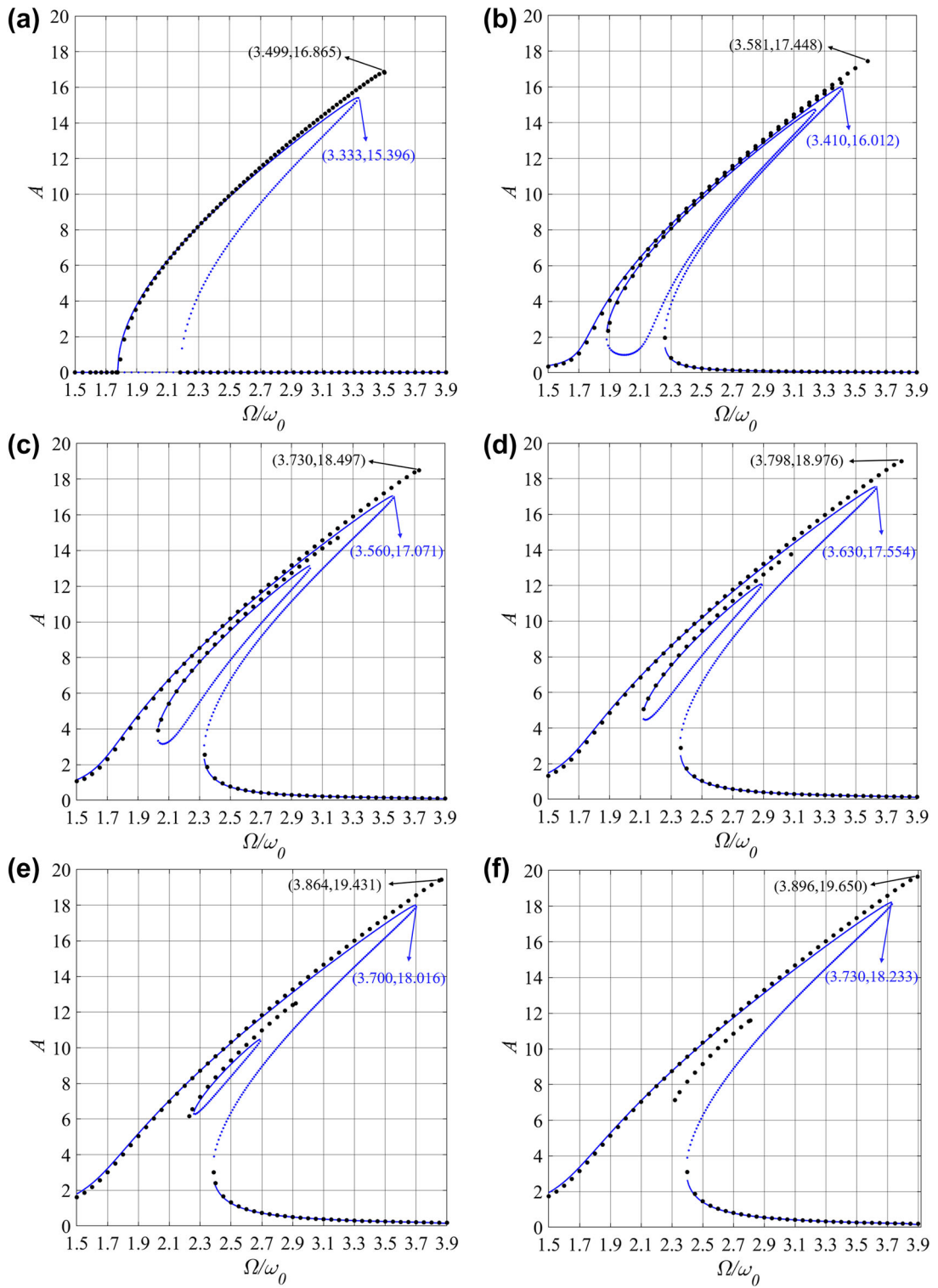
**Fig. 7** Frequency response diagrams illustrating the effect of adding external excitation of amplitude  $d$  on the amplitude of the responses of the system, comparing the results obtained from the single-term approximation of the MVA and numerical results obtained from DI. The blue-colored solid lines and discrete data points represent the stable and unstable results obtained from the single-term approximation of the MVA using Eq. (12), respectively, and black dots represent the numerical results obtained from DI; **a** the system under pure parametric excitation with no external excitation ( $d = 0$ ), **b** the parametrically excited system under interacting external excitation of amplitude  $d = 0.1$ , **c**  $d = 0.3$ , **d**  $d = 0.4$ , **e**  $d = 0.5$ , **f**  $d = 0.55$  ( $\beta = 0.15$ ,  $\eta = 0.01$ ,  $\omega_0 = 1$ ,  $P = 0.5$ ,  $\varphi = -\pi/4$ )

**Fig. 7** Frequency response diagrams illustrating the effect of adding external excitation of amplitude  $d$  on the amplitude of the responses of the system, comparing the results obtained from the single-term approximation of the MVA and numerical results obtained from DI. The blue-colored solid lines and discrete data points represent the stable and unstable results obtained from the single-term approximation of the MVA using Eq. (12), respectively, and black dots represent the numerical results obtained from DI; **a** the system under pure parametric excitation with no external excitation ( $d = 0$ ), **b** the parametrically excited system under interacting external excitation of amplitude  $d = 0.1$ , **c**  $d = 0.3$ , **d**  $d = 0.4$ , **e**  $d = 0.5$ , **f**  $d = 0.55$  ( $\beta = 0.15$ ,  $\eta = 0.01$ ,  $\omega_0 = 1$ ,  $P = 0.5$ ,  $\varphi = -\pi/4$ )

seen, the analytical results obtained from the expansions show good agreement with the results obtained directly from Eq. (12) for the whole frequency range considered, while those from Eqs. (41) and (42), which concern the upper bound responses and the corresponding frequencies, are accurate.

### 3 Results and discussion

In this section, we compare analytical and numerical results in detail and show the corresponding frequency



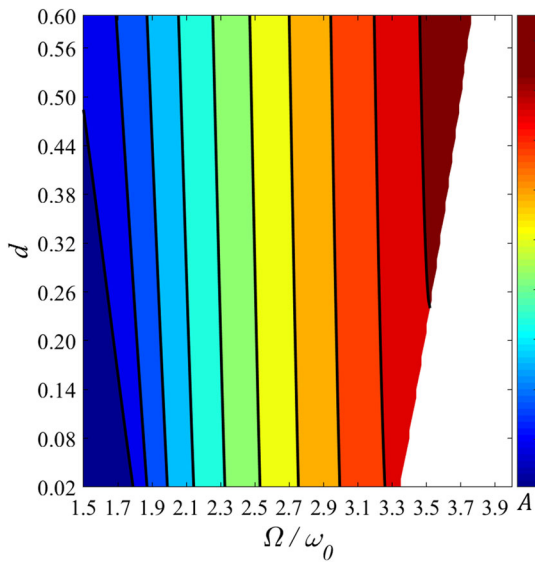


**Fig. 8**  $A$  as a function of  $d$  and  $\Omega/\omega_0$ , showing the results of the single-term approximation of the MVA for the upper stable branch b1 ( $\beta = 0.15$ ,  $\eta = 0.01$ ,  $\omega_0 = 1$ ,  $P = 0.5$ ,  $\varphi = -\pi/4$ )

response functions. We also compare our results with those found using the conventional Method of Multiple Scales (MMS), which is a perturbation method.

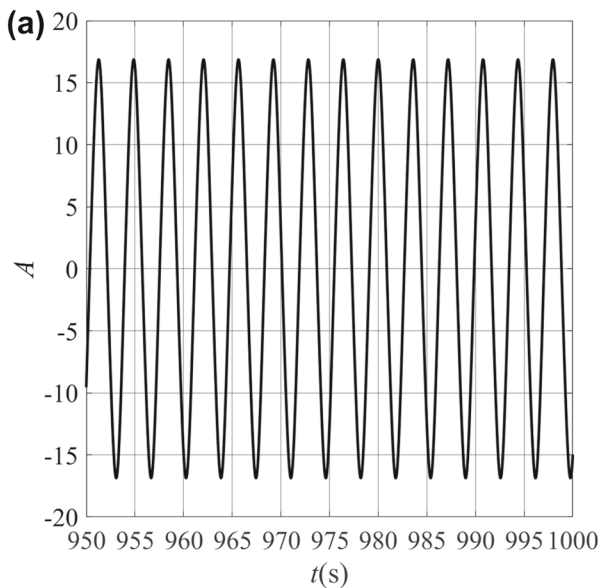
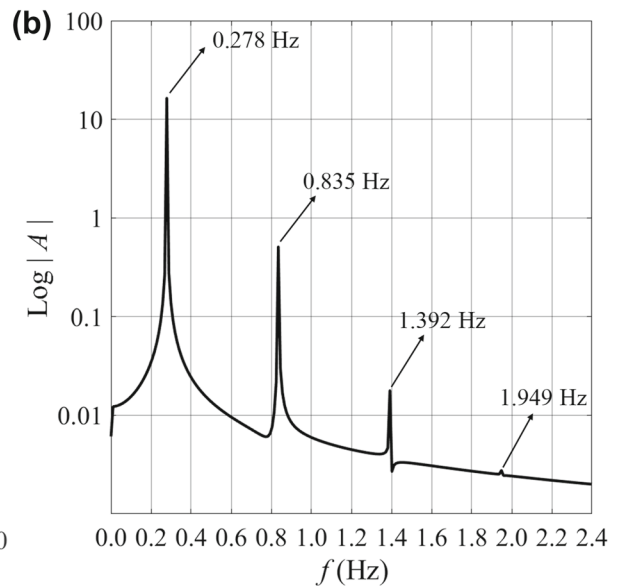


**Fig. 9** Numerically obtained response of the system at the upper bound frequency for the case where the system is under pure parametric excitation with no external excitation

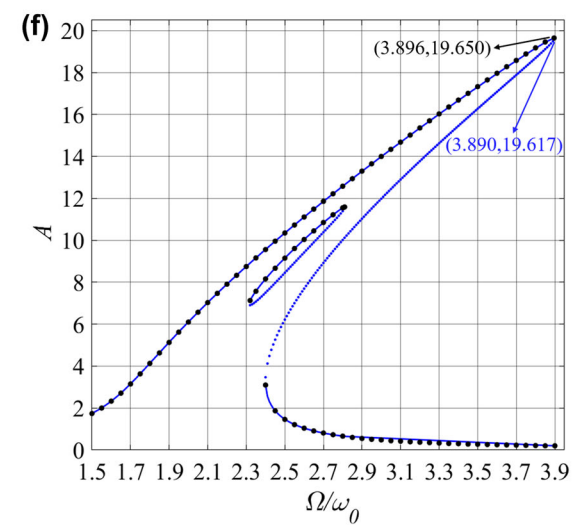
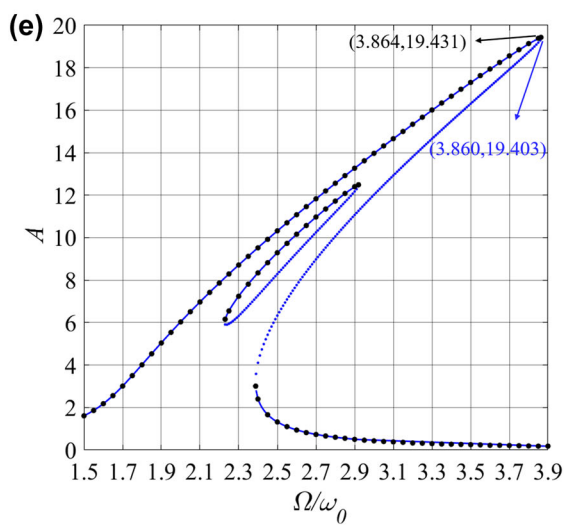
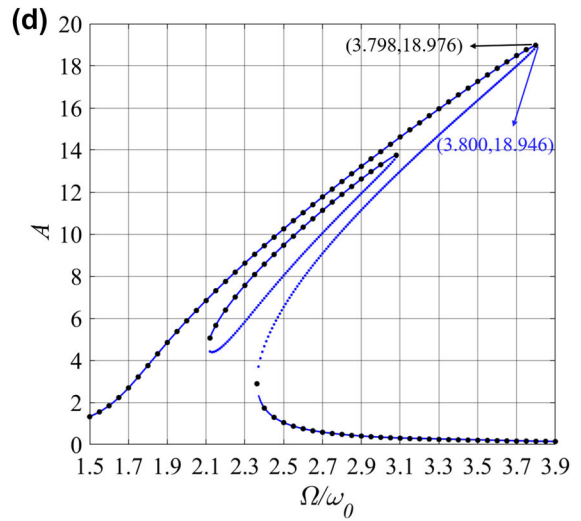
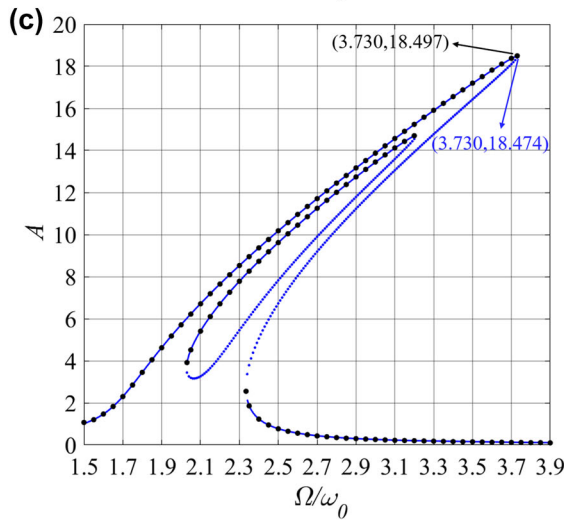
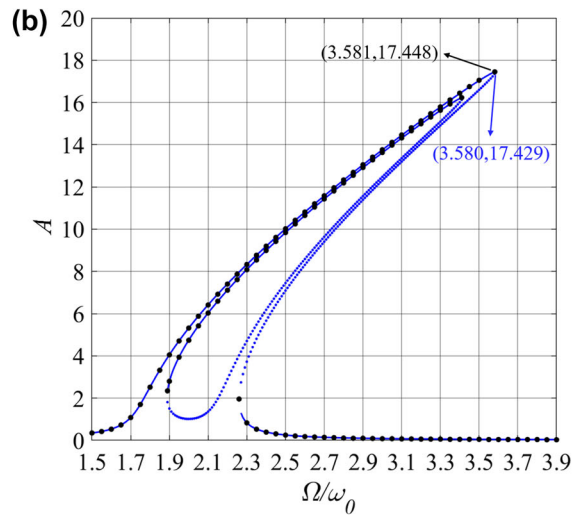
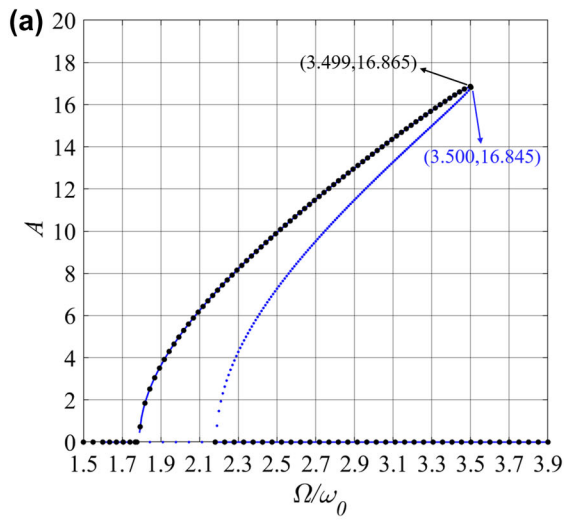
**Fig. 10** Frequency response diagrams for the system under interacting parametric and external excitations obtained from the double-term approximation of the MVA using Eqs. (20)-(23) and direct integration of the equation of motion. The blue solid lines and discrete data points represent the stable and unstable results obtained from the double-term approximation of the MVA, respectively, and black dots represent the numerical results obtained from DI; **a**  $d = 0$ , **b**  $d = 0.1$ , **c**  $d = 0.3$ , **d**  $d = 0.4$ , **e**  $d = 0.5$ , **f**  $d = 0.55$  ( $\beta = 0.15$ ,  $\eta = 0.01$ ,  $\omega_0 = 1$ ,  $P = 0.5$ ,  $\varphi = -\pi/4$ )

### 3.1 Single-term MVA approximation results

To investigate the accuracy of the analytical results obtained from the single-term approximation of the MVA, the amplitude response  $A$  of the system is depicted against the frequency ratio  $\Omega/\omega_0$  for various values of the external excitation amplitude  $d$  in Fig. 7. The cases where the system is under pure parametric excitation with no external excitation ( $d = 0$ ) and where the system is under interacting parametric and external excitations ( $d = 0.1$ ,  $d = 0.3$ ,  $d = 0.4$ ,  $d = 0.5$  and  $d = 0.55$ ) are shown. The results are compared with the results obtained by direct numerical integration (DI) of the equation of motion (1). As can be seen, the analytical results obtained from the single-term approximation of the MVA using (12) are in good



( $\Omega = 3.499$ ,  $A = 16.865$ ): **a** amplitude, **b** the FFT of the response ( $\beta = 0.15$ ,  $\eta = 0.01$ ,  $\omega_0 = 1$ ,  $P = 0.5$ )



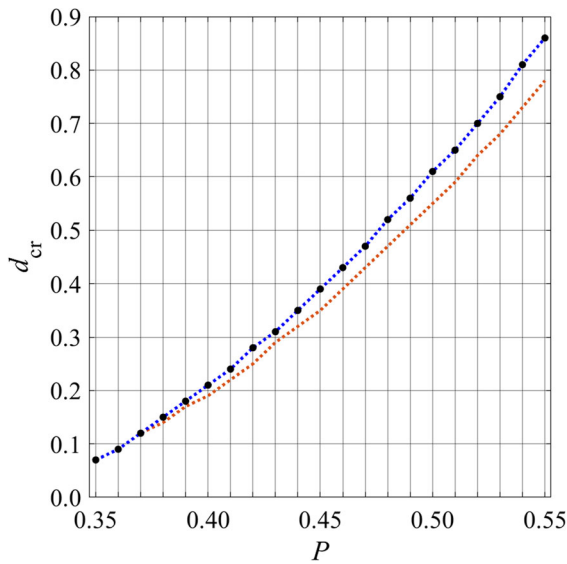


**Fig. 11** Critical values of the external excitation amplitude  $d_{cr}$  as a function of  $P$ , comparing the results obtained from the single-term approximation of the MVA (brown dotted line), the double-term approximation of the MVA (blue-dotted line), and the results obtained from DI (black dots) ( $\beta = 0.15$ ,  $\eta = 0.01$ ,  $\omega_0 = 1$ ,  $\varphi = -\pi/4$ )

agreement with the numerical results, showing a maximum deviation of 8.71% (for  $d = 0.55$ ).

For a small external excitation amplitude  $d$ , the upper bound excitation frequency and amplitude obtained from the expansion developed around this critical point using Eqs. (41) and (42) are in a good agreement with the MVA results obtained from the frequency response Eq. (12) (single-term approximation): for  $d = 0.1$ ,  $d = 0.3$  and  $d = 0.4$ ,  $A_{u2}$  is estimated to be 15.76 (at  $\Omega_{u2} = 3.42$ ), 18.64 (at  $\Omega_{u2} = 3.59$ ) and 21.17 (at  $\Omega_{u2} = 3.68$ ), respectively. However, for a larger value of  $d$ , the difference between the two results increases: for  $d = 0.5$  and  $d = 0.55$ ,  $A_{u2}$  from the expansion is estimated to be 24.42 (at  $\Omega_{u2} = 3.77$ ) and 26.31 (at  $\Omega_{u2} = 3.81$ ), respectively. The developed closed-form expressions (41) and (42) are very useful for designing PE systems with lower levels of direct excitation, so as to achieve maximum possible amplitude response.

The upper stable branch from the single-term approximation of the MVA (b1 in Fig. 1) is depicted against  $d$  and  $\Omega/\omega_0$  in Fig. 8. It can be seen that, for a fixed value of  $P$ , increasing  $d$  increases the frequency bandwidth and the upper bound to the response of the system. The response of the system is bounded, as is suggested both by the analytical results obtained from the single-term approximation of the MVA using Eq. (12) and the numerical simulations. Considering

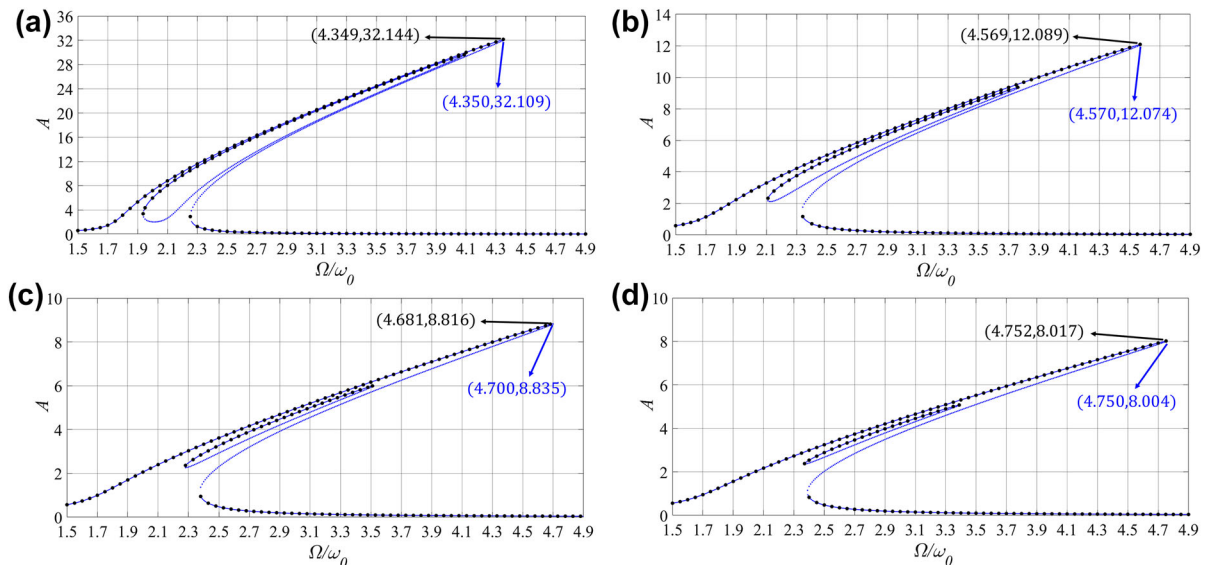


**Fig. 12** Response amplitude  $A$  as a function of frequency ratio  $\Omega/\omega_0$  for various values of the Duffing nonlinearity term  $\eta$ . Illustrating the results for the system under interacting parametric and external excitations obtained from the double-

term approximation of the MVA using Eqs. (20)-(23) (blue colored results) and direct integration of the equation of motion (black dots), **a**  $\eta = 0.005$ , **b**  $\eta = 0.04$ , **c**  $\eta = 0.08$ , **d**  $\eta = 0.1$  ( $\beta = 0.1$ ,  $\omega_0 = 1$ ,  $P = 0.4$ ,  $d = 0.2$ ,  $\varphi = -\pi/4$ )

the upper bound response obtained numerically for the system under pure parametric excitation with no external excitation (Fig. 7a), the time dependence of the response for this critical point ( $\Omega = 3.499$ ,  $A = 16.865$ ) and its Fast Fourier Transform (FFT) are presented in Fig. 9. (Note the logarithmic scale of the coordinate in Fig. 9b). As can be seen, four harmonics in the response are evident with frequencies that are equal to the first four frequencies ( $\Omega/2, 3\Omega/2, 5\Omega/2, 7\Omega/2$ ) of the MVA expansion. The first two harmonics are dominant. This implies that a more accurate approximation of the response can be obtained by using the double-term approximation of the MVA.

### 3.2 Double-term MVA approximation results

The results obtained from the double-term approximation of the MVA are compared with numerical results obtained from DI in Fig. 10. To make a direct comparison with the results obtained from the single-term MVA approximation, the system parameters are considered to be the same as those of Fig. 7. As suggested by the FFT of the upper bound response obtained numerically (Fig. 9), the double-term approximation of the MVA can predict the response of the system more accurately compared to the single-term approximation, with the frequency and amplitude of the upper bound showing a maximum of 0.2% difference from values found by direct numerical integration.

As can be seen in Figs. 7 and 10, increasing the external excitation amplitude, the two internal branches b2 and b3 (see Fig. 1) decrease in length and at a critical external excitation amplitude  $d_{cr}$  these branches will collapse. For the same set of system parameters, and for various values of  $P$ ,  $d_{cr}$  is depicted in Fig. 11, where the results for  $d_{cr}$  obtained from the single-term and double-term approximations of the MVA are presented and compared with the numerical results obtained from DI.

The analytical results obtained from the single-term MVA approximation using Eq. (12) and the double-term MVA approximation of Eqs. (20)–(23) show that the MVA is capable of predicting the bounded response accurately. Furthermore, the approximations are developed without involving commonly used restrictions such as the system parameters being small or the excitation frequency being close to the principal

parametric resonance frequency. For a different set of system parameters, frequency response diagrams for various values of the Duffing nonlinearity  $\eta$  are obtained by applying the double-term MVA approximation (Fig. 12). The results are verified by the results obtained from DI. As can be seen, as  $\eta$  increases, so does the upper bound frequency. As a result, the upper bound of the response of the system occurs at frequencies quite far from the principal parametric resonance frequency. Nevertheless, it can be seen that the MVA accurately predicts the upper bound frequency and amplitude. This is in contrast with conventional perturbation methods which cannot predict a bounded response and whose accuracy deteriorates for larger values of system parameters or as the excitation frequency increases [34].

### 3.3 Comparison with conventional perturbation methods

The conventional Method of Multiple Scales (MMS) is a commonly used perturbation method that has been applied to this problem. In this section, the first and second approximations of MMS are applied to the equation of motion (1) to obtain an approximate steady state response. Frequency response equations are developed, and results are compared with MVA results and numerical results obtained from DI.

#### 3.3.1 The first approximation of MMS

To the first approximation, the frequency response equation using the conventional MMS for the case when the system is under pure parametric excitation with no external excitation ( $d = 0$ ) is given by [34]

$$A = \sqrt{\frac{4\omega_0}{3\eta} \left( \Omega - 2\omega_0 \pm \sqrt{\left(\frac{1}{2}\omega_0 P\right)^2 - \beta^2} \right)}, \quad (43)$$

where, for positive  $\beta$  and  $\eta$ , the positive and negative signs represent the stable and unstable responses, respectively. Comparing Eq. (43) with Eq. (25), it can be seen that when applying the MVA a nontrivial stable solution exists only if  $\beta\Omega \leq \omega_0^2 P$ , while using the MMS this condition changes to  $2\beta \leq \omega_0 P$ , which does not depend on the excitation frequency  $\Omega$ . This is why the first-order approximation of the conventional MMS presented in Eq. (43) predicts an unbound

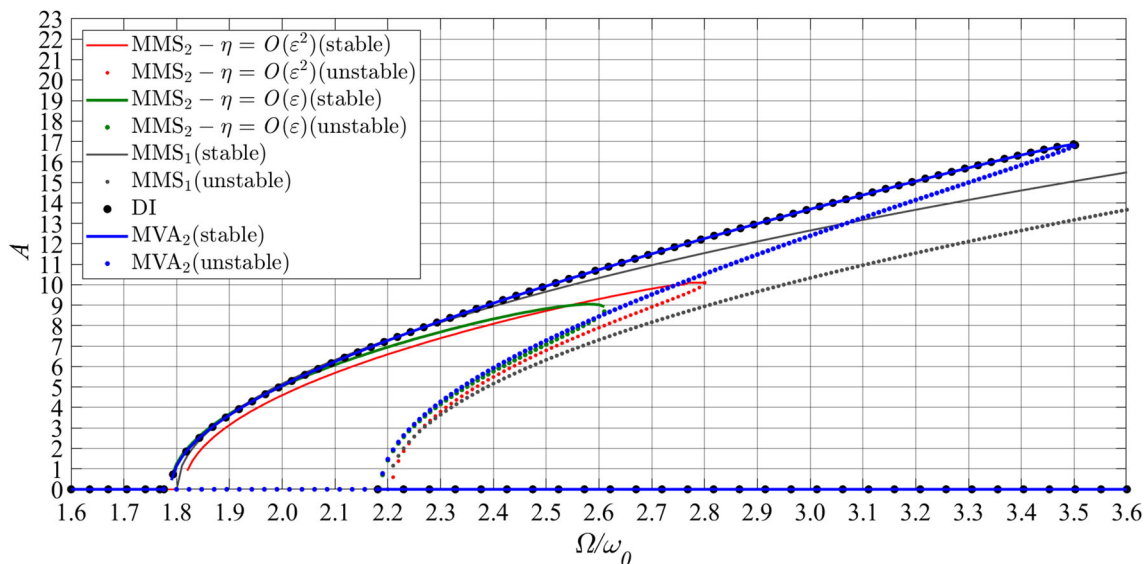


**Fig. 13** Response amplitude  $A$  as a function of  $\Omega/\omega_0$  for the system under pure parametric excitation with no external excitation ( $d = 0$ ), comparing the results obtained from the first approximation of the MMS, the second approximation of the

MMS for  $\eta = O(\varepsilon)$  using Eq. (44), the second approximation of the MMS for  $\eta = O(\varepsilon^2)$  using Eq. (46), the double-term approximation of the MVA using Eqs. (20)-(23), and numerical results obtained from DI ( $\beta = 0.15$ ,  $\eta = 0.01$ ,  $\omega_0 = 1$ ,  $P = 0.5$ )

response as  $\Omega$  increases. Note that a bounded response can also be predicted by the averaging method using the Mitropolskii technique [50], and, to the first approximation, the frequency response equation obtained by this method for a system under pure parametric excitation is identical to the one predicted by the single-term approximation of the MVA [34].

### 3.3.2 The second approximation of MMS

To develop the second approximation of MMS, two approaches are considered in this paper. While all the system parameters (except the Duffing nonlinearity term  $\eta$ ) are assumed to be small and of order  $O(\varepsilon)$ , where  $\varepsilon$  is a small bookkeeping parameter, in the first approach  $\eta$  also assumed to be  $O(\varepsilon)$ , while in the second approach  $\eta$  is assumed to be  $O(\varepsilon^2)$ , i.e., small compared to the other parameters. Frequency response equations are developed for both approaches and results are depicted for comparison.

**3.3.2.1 Case  $\eta = O(\varepsilon)$**  Applying the second-order approximation of the MMS, assuming the system parameters including the Duffing nonlinearity term  $\eta$  are all of order  $\varepsilon$ , the frequency response equation of the system under pure parametric excitation is obtained as (see Appendix A for details)

$$\left(\frac{k_1 + k_2A + k_3A^2}{k_4 + k_5A^2}\right)^2 + \left(\frac{k_6 + k_7A^2}{\frac{1}{2}k_4 + k_8A^2}\right)^2 = 1, \tag{44}$$

where the coefficients  $k_n$ ,  $n = 1, 2, \dots, 8$  are

$$\begin{aligned} k_1 &= \Omega - 2\omega_0 - \frac{1}{16}\omega_0P^2 - \frac{\omega_0^3P^2}{4\Omega(\Omega + 2\omega_0)} + \frac{1}{4\omega_0}\beta^2, \\ k_2 &= \frac{15}{128\omega_0^3}\eta^2, \quad k_3 = -\frac{3}{4\omega_0}\eta, \quad k_4 = -\frac{1}{4}P(\Omega - 4\omega_0), \\ k_5 &= \left(\frac{3\omega_0}{8\Omega(\Omega + 2\omega_0)} + \frac{1}{64\omega_0}\right)\eta P, \quad k_6 = -\frac{1}{2}\beta a, \\ k_7 &= \frac{3}{16\omega_0^2}\beta\eta, \\ k_8 &= \left(\frac{3\omega_0}{16\Omega(\Omega + 2\omega_0)} - \frac{13}{128\omega_0}\right)\eta P. \end{aligned} \tag{45}$$

**3.3.2.2 Case  $\eta = O(\varepsilon^2)$**  Alternatively, as another approximation, the frequency response equation can be obtained assuming the Duffing nonlinearity term  $\eta$  is of order  $\varepsilon^2$ , while the rest of the system parameters are assumed to be of order  $\varepsilon$ . Consequently, applying the second-order approximation of the MMS the frequency response equation becomes (see Appendix B for details)



$$\begin{aligned}
 & (12\eta\Omega(\Omega + 2\omega_0)A^2 - 16\omega_0\Omega^3 + \omega_0^2P^2\Omega^2 \\
 & - 4\beta^2\Omega(\Omega + 2\omega_0) + 64\Omega\omega_0^3 + 2P^2\omega_0^3(\Omega + 2\omega_0))^2 \quad (46) \\
 & + (16\beta\omega_0\Omega(\Omega + 2\omega_0))^2 \\
 & = (4P\omega_0\Omega(\Omega + 2\omega_0(\Omega - 4\omega_0)))^2.
 \end{aligned}$$

For the same set of system parameters as those of Figs. 7a and 10a, the results obtained from the first and second approximations of the MMS (MMS<sub>1</sub>, MMS<sub>2</sub>, respectively) are depicted in Fig. 13 and compared with the results obtained from the double-term approximation of the MVA (MVA<sub>2</sub>) and the numerical results obtained from DI. As can be seen, the first approximation of the MMS fails to predict a bounded response. Also, it is seen that when increasing the excitation frequency to a frequency range away from the principal parametric resonance ( $\Omega > 2\omega_0$ ), the accuracy of the predicted response decreases significantly compared to the numerical results and the analytical results obtained from the MVA. This is due to the fact that, when increasing the excitation frequency sufficiently above the principal parametric resonance frequency range, the frequency detuning parameter and the Duffing nonlinear term  $\eta u^3$  cannot be assumed to be small. Therefore, the results are valid only for a small frequency range around the principal parametric resonance (i.e., the frequency detuning parameter should be small). Furthermore, it can be seen that, using the second approximation of the MMS, one finds that the hardening Duffing-type nonlinearity results in the response being bounded around the principal parametric resonance, but the MMS fails to accurately predict the excitation frequency and the amplitude of the upper bound: the second approximations of the MMS for small  $\eta$  ( $O(\varepsilon)$ ) and very small  $\eta$  ( $O(\varepsilon^2)$ ) predict  $A_{u2} = 9.050$  (at  $\Omega_{u2} = 2.580$ ) and  $A_{u2} = 10.150$  (at  $\Omega_{u2} = 2.800$ ), respectively, while the predicted upper bound amplitude from the double-term MVA approximation and DI are  $A_{u2} = 16.845$  (at  $\Omega_{u2} = 3.500$ ) and  $A_{u2} = 16.865$  (at  $\Omega_{u2} = 3.499$ ), respectively.

Both frequency response equations developed for the second approximation of the MMS show that, unlike in most of the previous studies which claim that applying conventional MMS to a dynamical system as presented in Eq. (1) with linear damping cannot predict a bounded response, a bounded response can be achieved. This does not require nonlinear damping

to be introduced into the equation of motion or the frequency detuning parameter to be modified.

Figure 13 shows that, for the set of system parameters considered, the second approximation of the MMS developed assuming  $\eta = O(\varepsilon^2)$  predicts a wider frequency range compared to the results obtained assuming  $\eta = O(\varepsilon)$ . This is because here the value  $\eta = 0.01$  is used, which can be considered to be of order  $\varepsilon^2$ .

### 4 Conclusions

The response of nonlinear dynamical systems under interacting parametric and external excitations with a Duffing nonlinearity and linear damping was investigated in this paper. The paper focused on accurate prediction of the response of the system for a wide range of the system parameters. Closed-form analytical expressions for the upper bound response of the system and the corresponding frequency were obtained. These are relevant for applications.

The Method of Varying Amplitudes (MVA) was applied to the nonlinear forced Mathieu equation with linear damping. The case of hardening Duffing-type nonlinearity and a strict 2:1 frequency ratio between the parametric and external excitation frequencies was considered. The analytical results of the single-term approximation of the MVA showed that the response of the system is bounded, which was validated by numerical results obtained by Direct Integration (DI) of the equation of motion. The results are consistent with previous findings where bounded responses have been observed. Analytical expressions for the upper bound to the response of the system and the frequency at which it is attained were developed, and the results were illustrated for different cases, including the case where the system was under pure parametric excitation with no external excitation, and the case where the parametrically excited system was under an interacting external excitation of various amplitudes. Furthermore, the stability of the response was analyzed, and the results showed that, as expected, adding a small external disturbance to the pure parametrically excited system results in the stable/unstable nontrivial branches splitting into stable/unstable pairs due to degeneracy. As a result, a new internal loop will appear with a stable/unstable pair. Increasing the

external excitation amplitude, the internal loop becomes smaller and, for a critical value, it disappears.

By using the double-term MVA approximation, more accurate analytical results were derived and compared with the numerical results obtained by DI. The results showed that the double-term approximation of the MVA can accurately predict the response of the system. The analytical results were in good agreement with numerical results, showing a maximum of 0.2% deviation. Furthermore, the results are supported by observing the frequency spectrum of the system response.

It was shown that the first approximation of the conventional Method of Multiple Scales (MMS) does not predict a bounded response for the system considered. Additionally, the accuracy of the predictions decreases as the excitation frequency increases. This is because, for frequencies away from the principal parametric resonance frequency, the frequency detuning parameter and the Duffing nonlinear term cannot be assumed to be small. Therefore, the results of the first approximation of the MMS are valid only for a small frequency range around the principal parametric resonance. Also, it was seen that, using the second approximation of the MMS, the response around the principal parametric resonance is bounded. The characteristics of the upper bound response, however, cannot be accurately predicted using this approximation as the upper bound to the response of the system occurs in a frequency range away from the principal parametric resonance frequency. The results presented provide useful insights for the analysis and design of dynamical systems under interacting parametric and external excitations. Future work will consider experimental validation of analytical results in practical applications such as signal sensing, energy harvesting and response amplification.

**Author contributions** V.S. and B.M. conceived of, designed and supervised the study. M.A. performed the theoretical analysis including the numerical simulations and drafted the manuscript. All authors read, edited and approved the manuscript.

**Funding** The first author was supported by a Faculty of Engineering Doctoral Scholarship at the University of Auckland.

## Declarations

**Conflict of interest** The authors declare that they have no conflict of interest.

## Appendix A: second approximation of MMS assuming Duffing nonlinearity term $\eta$ to be $O(\varepsilon)$

In Appendix, results from the second-order MMS are briefly reviewed [33]. To obtain the frequency response equation of a dynamical system under pure parametric excitation with no external excitation ( $d = 0$ ) using the MMS, assuming the system parameters including the Duffing nonlinearity term are all small and of order  $\varepsilon$ , we express Eq. (1) as

$$\ddot{u} + \varepsilon\beta_\varepsilon\dot{u} + \omega_0^2(1 + \varepsilon P_\varepsilon \cos(\Omega t))u + \varepsilon\eta_\varepsilon u^3 = 0, \quad (\text{A1})$$

where

$$\varepsilon\beta_\varepsilon = \beta, \quad \varepsilon P_\varepsilon = P, \quad \varepsilon\eta_\varepsilon = \eta. \quad (\text{A2})$$

To the second approximation of the MMS, the response of the system can be written as [33]

$$u(T_0, T_1, T_2) = u_0(T_0, T_1, T_2) + \varepsilon u_1(T_0, T_1, T_2) + \varepsilon^2 u_2(T_0, T_1, T_2) + O(\varepsilon^3), \quad (\text{A3})$$

where  $T_0 = t$ ,  $T_1 = \varepsilon t$  and  $T_2 = \varepsilon^2 t$  are time scales. Defining the operator

$$D_n = \frac{\partial}{\partial T_n}, \quad n = 0, 1, 2, \dots, \quad (\text{A4})$$

the time derivatives can be expressed as

$$\frac{d}{dt} = D_0 + \varepsilon D_1 + \varepsilon^2 D_2 + O(\varepsilon^3), \quad (\text{A5})$$

$$\frac{d^2}{dt^2} = D_0^2 + 2\varepsilon D_0 D_1 + \varepsilon^2 (2D_0 D_1 + D_1^2) + O(\varepsilon^3), \quad (\text{A6})$$

Substituting Eq. (A3) into Eq. (A1), considering Eqs. (A4)–(A6) and equating coefficients of like powers of  $\varepsilon$ , we obtain

$$O(1): D_0^2 u_0 + \omega_0^2 u_0 = 0, \quad (\text{A7})$$

$$\begin{aligned}
 O(\varepsilon) : D_0^2 u_1 + \omega_0^2 u_1 &= -2D_0 D_1 u_0 - \beta_\varepsilon D_0 u_0 - \eta_\varepsilon u_0^3 \\
 &\quad - \frac{1}{2} \omega_0^2 P_\varepsilon (e^{i\Omega T_0} + e^{-i\Omega T_0}) u_0, \tag{A8}
 \end{aligned}$$

$$\begin{aligned}
 O(\varepsilon^2) : D_0^2 u_2 + \omega_0^2 u_2 &= -D_1^2 u_0 - 2D_0 D_2 u_0 \\
 &\quad - 2D_0 D_1 u_1 - 3\eta_\varepsilon u_0^2 u_1 \\
 &\quad - \beta_\varepsilon (D_1 u_0 + D_0 u_1) - \frac{1}{2} \omega_0^2 P_\varepsilon (e^{i\Omega T_0} + e^{-i\Omega T_0}) u_1. \tag{A9}
 \end{aligned}$$

The solution of Eq. (A7) is assumed to be of the form

$$u_0 = A(T_1, T_2) e^{i\omega_0 T_0} + \bar{A}(T_1, T_2) e^{-i\omega_0 T_0}, \tag{A10}$$

where  $\bar{A}(T_1, T_2)$  is the complex conjugate of  $A(T_1, T_2)$ . Substituting Eq. (A10) into Eq. (A8), we obtain

$$\begin{aligned}
 D_0^2 u_1 + \omega_0^2 u_1 &= (-2i\omega_0 D_1 A - i\omega_0 \beta_\varepsilon A \\
 &\quad - \frac{1}{2} \omega_0^2 P_\varepsilon \bar{A} e^{i(\Omega-2\omega_0)T_0} - 3\eta_\varepsilon A^2 \bar{A}) e^{i\omega_0 T_0} \\
 &\quad - \frac{1}{2} \omega_0^2 P_\varepsilon A e^{i(\Omega+\omega_0)T_0} - \eta_\varepsilon A^3 e^{3i\omega_0 T_0} + CC, \tag{A11}
 \end{aligned}$$

where CC is the complex conjugate of the preceding terms. Considering  $\Omega \approx 2\omega_0$ , the coefficients of  $\exp(i\omega_0 T_0)$  in Eq. (A11) represent the secular terms which can be eliminated when

$$D_1 A = -\frac{1}{2} \beta_\varepsilon A + \frac{i}{4} \omega_0 P_\varepsilon \bar{A} e^{i(\Omega-2\omega_0)T_0} + \frac{3i}{2\omega_0} \eta_\varepsilon A^2 \bar{A}. \tag{A12}$$

Consequently, the particular solution of  $u_1$  in Eq. (A11) is obtained as

$$\begin{aligned}
 u_1 &= \frac{\omega_0^2 P_\varepsilon A}{2\Omega(\Omega + 2\omega_0)} e^{i(\Omega+\omega_0)T_0} + \frac{1}{8\omega_0^2} \eta_\varepsilon A^3 e^{3i\omega_0 T_0} \\
 &\quad + CC. \tag{A13}
 \end{aligned}$$

Substituting  $u_0$  and  $u_1$  from Eqs. (A10) and (A13) into Eq. (A9), we obtain

$$\begin{aligned}
 D_0^2 u_2 + \omega_0^2 u_2 &= \left( -D_1^2 A - \beta_\varepsilon D_1 A - 2i\omega_0 D_2 A - \frac{\omega_0^4 P_\varepsilon^2 A}{4\Omega(\Omega + 2\omega_0)} \right. \\
 &\quad - \frac{3}{8\omega_0^2} \eta_\varepsilon^2 \bar{A}^2 A^3 - \frac{3\omega_0^2 \eta_\varepsilon P_\varepsilon A \bar{A}^2}{2\Omega(\Omega + 2\omega_0)} e^{i(\Omega-2\omega_0)T_0} \\
 &\quad \left. - \frac{1}{16} \eta_\varepsilon P_\varepsilon A^3 e^{-i(\Omega-2\omega_0)T_0} \right) e^{i\omega_0 T_0} \\
 &\quad + \text{NST} + \text{CC} \tag{A14}
 \end{aligned}$$

where NST denotes the non-secular terms. Defining a frequency detuning parameter  $\sigma$  such that

$$\Omega - 2\omega_0 = \varepsilon\sigma, \tag{A15}$$

eliminating the secular terms in Eq. (A14) give

$$\begin{aligned}
 D_1^2 A &= -\beta_\varepsilon D_1 A - 2i\omega_0 D_2 A - \frac{\omega_0^4 P_\varepsilon^2 A}{4\Omega(\Omega + 2\omega_0)} \\
 &\quad - \frac{3}{8\omega_0^2} \eta_\varepsilon^2 \bar{A}^2 A^3 - \frac{3\omega_0^2 \eta_\varepsilon P_\varepsilon A \bar{A}^2}{2\Omega(\Omega + 2\omega_0)} e^{i\sigma T_1} \\
 &\quad - \frac{1}{16} \eta_\varepsilon P_\varepsilon A^3 e^{-i\sigma T_1}. \tag{A16}
 \end{aligned}$$

Furthermore, Eq. (A12) can be rewritten as

$$\begin{aligned}
 D_1^2 A &= \frac{1}{16} A (\omega_0^2 P_\varepsilon^2 + 4\beta_\varepsilon^2) - \frac{3i}{\omega_0} \beta_\varepsilon \eta_\varepsilon A^2 \bar{A} - \frac{9}{4\omega_0^2} \eta_\varepsilon^2 A^3 \bar{A}^2 \\
 &\quad - \left( \frac{i}{4} \omega_0 \beta_\varepsilon P_\varepsilon \bar{A} + \frac{1}{4} \omega_0 P_\varepsilon \sigma \bar{A} + \frac{3}{8} \eta_\varepsilon P_\varepsilon A \bar{A}^2 \right) e^{i\sigma T_1} \\
 &\quad + \frac{3}{8} \eta_\varepsilon P_\varepsilon A^3 e^{-i\sigma T_1}. \tag{A17}
 \end{aligned}$$

Also, from Eq. (A16) and considering Eq. (12) we obtain

$$\begin{aligned}
 D_1^2 A &= \frac{1}{2} \beta_\varepsilon^2 A - \frac{3i}{2\omega_0} \beta_\varepsilon \eta_\varepsilon A^2 \bar{A} - 2i\omega_0 D_2 A - \frac{\omega_0^4 P_\varepsilon^2 A}{4\Omega(\Omega + 2\omega_0)} \\
 &\quad - \frac{3}{8\omega_0^2} \eta_\varepsilon^2 A^3 \bar{A}^2 - \left( \frac{i}{4} \omega_0 \beta_\varepsilon P_\varepsilon \bar{A} + \frac{3\omega_0^2 \eta_\varepsilon P_\varepsilon A \bar{A}^2}{2\Omega(\Omega + 2\omega_0)} \right) e^{i\sigma T_1} \\
 &\quad - \frac{1}{16} \eta_\varepsilon P_\varepsilon A^3 e^{-i\sigma T_1}. \tag{A18}
 \end{aligned}$$

Combining Eqs. (A17) and (A18) and cancelling  $D_1^2 A$  give

$$2i\omega_0 D_2 A = \frac{1}{4} \beta_\varepsilon^2 A - \frac{1}{16} \omega_0^2 P_\varepsilon^2 A - \frac{\omega_0^4 P_\varepsilon^2 A}{4\Omega(\Omega + 2\omega_0)} + \frac{3i}{2\omega_0} \beta_\varepsilon \eta_\varepsilon A^2 \bar{A} + \frac{15}{8\omega_0^2} \eta_\varepsilon^2 A^3 \bar{A}^2 + \left( \frac{1}{4} \omega_0 P_\varepsilon \sigma \bar{A} + \frac{3}{8} \eta_\varepsilon P_\varepsilon A \bar{A}^2 - \frac{3\omega_0^2 \eta_\varepsilon P_\varepsilon A \bar{A}^2}{2\Omega(\Omega + 2\omega_0)} \right) e^{i\sigma T_1} - \frac{7}{16} \eta_\varepsilon P_\varepsilon A^3 e^{-i\sigma T_1}. \tag{A19}$$

Multiplying Eq. (A12) by  $2i\omega_0\varepsilon$  and Eq. (A19) by  $\varepsilon^2$  and combining the resulting equations yield

$$2i\omega_0(\varepsilon D_1 A + \varepsilon^2 D_2 A) + \varepsilon \left( i\omega_0 \beta_\varepsilon A + \frac{1}{2} \omega_0^2 P_\varepsilon \bar{A} e^{i\sigma T_1} + 3\eta_\varepsilon A^2 \bar{A} \right) + \varepsilon^2 \left( \frac{1}{16} \omega_0^2 P_\varepsilon^2 A + \frac{\omega_0^4 P_\varepsilon^2 A}{4\Omega(\Omega + 2\omega_0)} - \frac{1}{4} \beta_\varepsilon^2 A - \frac{3i}{2\omega_0} \beta_\varepsilon \eta_\varepsilon A^2 \bar{A} - \frac{15}{8\omega_0^2} \eta_\varepsilon^2 A^3 \bar{A}^2 - \frac{1}{4} \omega_0 P_\varepsilon \sigma \bar{A} e^{i\sigma T_1} - \frac{3}{8} \eta_\varepsilon P_\varepsilon A \bar{A}^2 e^{i\sigma T_1} + \frac{3\omega_0^2 \eta_\varepsilon P_\varepsilon A \bar{A}^2}{2\Omega(\Omega + 2\omega_0)} e^{i\sigma T_1} + \frac{7}{16} \eta_\varepsilon P_\varepsilon A^3 e^{-i\sigma T_1} \right) = 0. \tag{A20}$$

Taking Eq. (A2) into account, Eq. (A20) can be rewritten as

$$2i\omega_0 \frac{dA}{dt} - \frac{1}{4} \omega_0 P \bar{A} (\Omega - 4\omega_0) e^{i(\Omega - 2\omega_0)t} - \frac{1}{4} \beta^2 A + i\omega_0 \beta A + 3\eta A^2 \bar{A} + \frac{1}{16} \omega_0^2 p^2 A + \frac{\omega_0^4 p^2 A}{4\Omega(\Omega + 2\omega_0)} - \frac{3i}{2\omega_0} \beta \eta A^2 \bar{A} - \frac{15}{8\omega_0^2} \eta^2 A^3 \bar{A}^2 + \left( \frac{3\omega_0^2}{2\Omega(\Omega + 2\omega_0)} - \frac{3}{8} \right) \eta P A \bar{A}^2 e^{i(\Omega - 2\omega_0)t} + \frac{7}{16} \eta P A^3 e^{-i(\Omega - 2\omega_0)t} = 0, \tag{A21}$$

where  $A$  is a function of time and can be expressed in a polar form

$$A(t) = \frac{1}{2} a(t) e^{i\lambda(t)}, \tag{A22}$$

where  $a(t)$  and  $\lambda(t)$  are real. substituting Eq. (A22) into Eq. (A21), we obtain

$$-256\omega_0 a \dot{\lambda} + \left( \omega_0^2 p^2 + \frac{32\omega_0^4 p^2}{\Omega(\Omega + 2\omega_0)} - 32\beta^2 \right) a + 96\eta a^3 - \frac{15}{\omega_0^2} \eta^2 a^5 + i \left( 256\omega_0 \dot{a} + 128\omega_0 \beta a - \frac{48}{\omega_0} \beta \eta a^3 \right) + \left( \left( \frac{48\omega_0^2}{\Omega(\Omega + 2\omega_0)} - 12 \right) \eta P a^3 - 32\omega_0 P (\Omega - 4\omega_0) a \right) e^{i((\Omega - 2\omega_0)t - 2\lambda)} + 14\eta P a^3 e^{-i((\Omega - 2\omega_0)t - 2\lambda)} = 0. \tag{A23}$$

Applying the transformation

$$\tau(t) = (\Omega - 2\omega_0)t - 2\lambda(t) \tag{A24}$$

into Eq. (A23) and separating the resultant real and imaginary parts, the system of equations

$$a\dot{\tau} = \left( \Omega - 2\omega_0 - \frac{1}{16} \omega_0 p^2 - \frac{\omega_0^3 p^2}{4\Omega(\Omega + 2\omega_0)} + \frac{1}{4\omega_0} \beta^2 \right) a + \frac{15}{128\omega_0^3} \eta^2 a^2 - \frac{3}{4\omega_0} \eta a^3 - \left( \left( \frac{3\omega_0}{8\Omega(\Omega + 2\omega_0)} + \frac{1}{64\omega_0} \right) \eta P a^3 - \frac{1}{4} P (\Omega - 4\omega_0) a \right) \cos(\tau) = 0, \tag{A25}$$

$$\dot{a} = -\frac{1}{2} \beta a + \frac{3}{16\omega_0^2} \beta \eta a^3 - \left( \left( \frac{3\omega_0}{16\Omega(\Omega + 2\omega_0)} - \frac{13}{128\omega_0} \right) \eta P a^3 - \frac{1}{8} P (\Omega - 4\omega_0) a \right) \sin(\tau), \tag{A26}$$

is obtained. Consequently, solving Eqs. (A25) and (A26) for the steady state ( $\dot{a} = \dot{\tau} = 0$ ), the frequency response Eq. (44) is obtained (with symbol  $a$  replaced by  $A$  for consistency with the results obtained by the MVA).

### Appendix B: second approximation of MMS assuming Duffing nonlinearity $\eta$ to be $O(\varepsilon^2)$

To the second approximation of the MMS, assuming  $\eta$  is of order  $\varepsilon^2$ , the equation of motion is scaled as

$$\ddot{u} + \varepsilon \beta_\varepsilon \dot{u} + \omega_0^2 (1 + \varepsilon P_\varepsilon \cos(\Omega t)) u + \varepsilon^2 \eta_\varepsilon u^3 = 0, \tag{B1}$$

where  $\varepsilon^2 \eta_\varepsilon = \eta$ . Considering the system parameters to be of different orders of  $\varepsilon$  has been used commonly in the literature for various problems [25, 32, 33]. Here,  $\eta_\varepsilon$  is considered to be of order  $\varepsilon^2$ , which only implies the degree of smallness for Duffing nonlinearity. Considering Eqs. (A3)–(A6) and following a similar approach, Eq. (A7) still holds true for coefficients of order  $\varepsilon^0$ , while the equations representing coefficients of order  $\varepsilon$  and  $\varepsilon^2$  change to

$$D_0^2 u_1 + \omega_0^2 u_1 = -2D_0 D_1 u_0 - \beta_\varepsilon D_0 u_0 - \frac{1}{2} \omega_0^2 P_\varepsilon (e^{i\Omega T_0} + e^{-i\Omega T_0}) u_0, \tag{B2}$$

$$D_0^2 u_2 + \omega_0^2 u_2 = -D_1^2 u_0 - 2D_0 D_2 u_0 - 2D_0 D_1 u_1 - \beta_\varepsilon (D_1 u_0 + D_0 u_1) - \frac{1}{2} \omega_0^2 P_\varepsilon (e^{i\Omega T_0} + e^{-i\Omega T_0}) u_1 - \eta_\varepsilon u_0^3, \tag{B3}$$

respectively. The particular solution for  $u_1$  in Eq. (B2) is

$$u_1 = \frac{\omega_0^2 P_\varepsilon A}{2\Omega(\Omega + 2\omega_0)} e^{i(\Omega + \omega_0)T_0} + CC. \tag{B4}$$

Following an approach similar to that of Eqs. (A14)–(A22) in Appendix A, the modulation equation is obtained as

$$12\eta a^3 - 4\omega_0 P a (\Omega - 4\omega_0) e^{i((\Omega - 2\omega_0)t - 2\lambda)} + 32i\omega_0 \dot{a} + 16i\omega_0 \beta a + \omega_0^2 p^2 a + \frac{4\omega_0^4 p^2 a}{\Omega(\Omega + 2\omega_0)} - 4\beta^2 a - 32a\omega_0 \dot{\lambda} = 0. \tag{B5}$$

Consequently, applying the transformation (A24), the system of equations

$$a\dot{\tau} = a(\Omega - 2\omega_0) - \frac{3\eta a^3}{4\omega_0} - \frac{1}{16} \omega_0 p^2 a - \frac{\omega_0^3 p^2 a}{4\Omega(\Omega + 2\omega_0)} + \frac{1}{4} \beta^2 a + \frac{1}{2} P a (\Omega - 4\omega_0) \cos(\tau), \tag{B6}$$

$$\dot{a} = -\frac{1}{2} \beta a + \frac{1}{8} P a (\Omega - 4\omega_0) \sin(\tau), \tag{B7}$$

is obtained. Solving Eqs. (B6) and (B7) for the steady state ( $\dot{a} = \dot{\tau} = 0$ ), the frequency response Eq. (46) is obtained (with symbol  $a$  replaced by  $A$  for consistency with the results obtained by the MVA).

**References**

1. Wu, Z., Xie, C., Mei, G., Dong, H.: Dynamic analysis of parametrically excited marine riser under simultaneous stochastic waves and vortex. *Adv. Struct. Eng.* **22**, 268–283 (2018)

2. Zhou, L., Chen, F.: Chaotic motion of the parametrically excited roll motion for a class of ships in regular longitudinal waves. *Ocean Eng.* **195**, 106729 (2020)

3. Thompson, J., Rainey, R., Soliman, M.: Mechanics of ship capsizing under direct and parametric wave excitation. *Philos. Trans. R. Soc. Lond. Ser. A Phys. Eng. Sci.* **338**, 471–490 (1992)

4. Gonzalez-Buelga, A., Neild, S., Wagg, D., Macdonald, J.: Modal stability of inclined cables subjected to vertical support excitation. *J. Sound Vib.* **318**, 565–579 (2008)

5. Peng, J., Xiang, M., Wang, L., Xie, X., Sun, H., Yu, J.: Nonlinear primary resonance in vibration control of cable-stayed beam with time delay feedback. *Mech. Syst. Signal Process.* **137**, 106488 (2020)

6. Torteman, B., Kessler, Y., Liberzon, A., Krylov, S.: Micro-beam resonator parametrically excited by electro-thermal Joule’s heating and its use as a flow sensor. *Nonlinear Dyn.* **98**, 3051–3065 (2019)

7. Meesala, V., Hajj, M.: Parameter sensitivity of cantilever beam with tip mass to parametric excitation. *Nonlinear Dyn.* **95**, 3375–3384 (2019)

8. Zhang, W., Turner, K.: Application of parametric resonance amplification in a single-crystal silicon micro-oscillator based mass sensor. *Sens. Actuat. A Phys.* **122**, 23–30 (2005)

9. Xia, G., Fang, F., Zhang, M., Wang, Q., Wang, J.: Performance analysis of parametrically and directly excited nonlinear piezoelectric energy harvester. *Arch. Appl. Mech.* **89**, 2147–2166 (2019)

10. Jia, Y., Yan, J., Soga, K., Seshia, A.: Parametrically excited MEMS vibration energy harvesters with design approaches to overcome the initiation threshold amplitude. *J. Micromech. Microeng.* **23**, 114007 (2013)

11. Yildirim, T., Ghayesh, M., Li, W., Alici, G.: Design and development of a parametrically excited nonlinear energy harvester. *Energy Conv. Manag.* **126**, 247–255 (2016)

12. Alevras, P., Theodossiadis, S., Rahnejat, H.: Broadband energy harvesting from parametric vibrations of a class of nonlinear Mathieu systems. *Appl. Phys. Lett.* **110**, 233901 (2017)

13. Kuang, Y., Zhu, M.: Parametrically excited nonlinear magnetic rolling pendulum for broadband energy harvesting. *Appl. Phys. Lett.* **114**, 203903 (2019)

14. Dotti, F., Reguera, F., Machado, S.: Damping in a parametric pendulum with a view on energy harvesting. *Mech. Res. Commun.* **81**, 11–16 (2017)

15. Abdelkefi, A., Nayfeh, A., Hajj, M.: Global nonlinear distributed-parameter model of parametrically excited piezoelectric energy harvesters. *Nonlinear Dyn.* **67**, 1147–1160 (2011)

16. He, X., Rafiee, M., Mareishi, S.: Nonlinear dynamics of piezoelectric nanocomposite energy harvesters under parametric resonance. *Nonlinear Dyn.* **79**, 1863–1880 (2014)

17. Kumar, R., Gupta, S., Ali, S.: Energy harvesting from chaos in base excited double pendulum. *Mech. Syst. Signal Process.* **124**, 49–64 (2019)

18. Nabholz, U., Lamprecht, L., Mehner, J., Zimmermann, A., Degenfeld-Schonburg, P.: Parametric amplification of broadband vibrational energy harvesters for energy-autonomous sensors enabled by field-induced striction. *Mech. Syst. Signal Process.* **139**, 106642 (2020)

19. Garg, A., Dwivedy, S.: Dynamic analysis of piezoelectric energy harvester under combination parametric and internal resonance: a theoretical and experimental study. *Nonlinear Dyn.* **101**, 2107–2129 (2020)
20. Zorin, A.: Flux-driven Josephson traveling-wave parametric amplifier. *Phys. Rev. Appl.* **12**, 044051 (2019)
21. Rhoads, J., Shaw, S.: The impact of nonlinearity on degenerate parametric amplifiers. *Appl. Phys. Lett.* **96**, 234101 (2010)
22. Dolev, A., Bucher, I.: Experimental and numerical validation of digital, electromechanical, parametrically excited amplifiers. *J. Vib. Acoust.* **138**, 061001 (2016)
23. Jäckel, P., Mullin, T.: A numerical and experimental study of codimension-2 points in a parametrically excited double pendulum. *Proc. R. Soc. Lond. Ser. A Math. Phys. Eng. Sci.* **454**, 3257–3274 (1998)
24. Sorokin, V.: On the unlimited gain of a nonlinear parametric amplifier. *Mech. Res. Commun.* **62**, 111–116 (2014)
25. Dolev, A., Bucher, I.: Optimizing the dynamical behavior of a dual-frequency parametric amplifier with quadratic and cubic nonlinearities. *Nonlinear Dyn.* **92**, 1955–1974 (2018)
26. Sah, S., Mann, B.: Transition curves in a parametrically excited pendulum with a force of elliptic type. *Proc. R. Soc. A Math. Phys. Eng. Sci.* **468**, 3995–4007 (2012)
27. Peruzzi, N., Chavarette, F., Balthazar, J., Tusset, A., Pertierrari, A., Brasil, R.: The dynamic behavior of a parametrically excited time-periodic MEMS taking into account parametric errors. *J. Vib. Control.* **22**, 4101–4110 (2016)
28. Huang, Y., Fu, J., Liu, A.: Dynamic instability of Euler-Bernoulli nanobeams subject to parametric excitation. *Comp. B Eng.* **164**, 226–234 (2019)
29. Mao, X., Ding, H., Chen, L.: Parametric resonance of a translating beam with pulsating axial speed in the supercritical regime. *Mech. Res. Commun.* **76**, 72–77 (2016)
30. Rhoads, J., Shaw, S., Turner, K., Moehlis, J., DeMartini, B., Zhang, W.: Generalized parametric resonance in electrostatically actuated microelectromechanical oscillators. *J. Sound Vib.* **296**, 797–829 (2006)
31. Rhoads, J., Shaw, S., Turner, K.: The nonlinear response of resonant microbeam systems with purely-parametric electrostatic actuation. *J. Micromech. Microeng.* **16**, 890–899 (2006)
32. Shibata, A., Ohishi, S., Yabuno, H.: Passive method for controlling the nonlinear characteristics in a parametrically excited hinged-hinged beam by the addition of a linear spring. *J. Sound Vib.* **350**, 111–122 (2015)
33. Nayfeh, A., Mook, D.: *Nonlinear Oscillations*. Wiley, New York (1979)
34. Aghamohammadi, M., Sorokin, V., Mace, B.: On the response attainable in nonlinear parametrically excited systems. *Appl. Phys. Lett.* **115**, 154102 (2019)
35. Chen, S., Epureanu, B.: Forecasting bifurcations in parametrically excited systems. *Nonlinear Dyn.* **91**, 443–457 (2017)
36. Warminski, J.: Nonlinear dynamics of self-, parametric, and externally excited oscillator with time delay: van der Pol versus Rayleigh models. *Nonlinear Dyn.* **99**, 35–56 (2019)
37. Warminski, J.: Frequency locking in a nonlinear MEMS oscillator driven by harmonic force and time delay. *Int. J. Dyn. Control.* **3**, 122–136 (2015)
38. Li, D., Shaw, S.: The effects of nonlinear damping on degenerate parametric amplification. *Nonlinear Dyn.* **102**, 2433–2452 (2020)
39. Zaitsev, S., Shtempluck, O., Buks, E., Gottlieb, O.: Nonlinear damping in a micromechanical oscillator. *Nonlinear Dyn.* **67**, 859–883 (2011)
40. Gutschmidt, S., Gottlieb, O.: Nonlinear dynamic behavior of a microbeam array subject to parametric actuation at low, medium and large DC-voltages. *Nonlinear Dyn.* **67**, 1–36 (2010)
41. Szabelski, K., Warminski, J.: Self-excited system vibrations with parametric and external excitations. *J. Sound Vib.* **187**, 595–607 (1995)
42. Szabelski, K., Warmański, J.: Parametric self-excited nonlinear system vibrations analysis with inertial excitation. *Int. J. Non-Linear Mech.* **30**, 179–189 (1995)
43. Szabelski, K., Warmański, J.: Vibration of a non-linear self-excited system with two degrees of freedom under external and parametric excitation. *Nonlinear Dyn.* **14**, 23–36 (1997)
44. Sorokin, V., Thomsen, J.: Vibration suppression for strings with distributed loading using spatial cross-section modulation. *J. Sound Vib.* **335**, 66–77 (2015)
45. Neumeier, S., Sorokin, V., van Gestel, M., Thomsen, J.: Frequency detuning effects for a parametric amplifier. *J. Sound Vib.* **445**, 77–87 (2019)
46. Aghamohammadi, M., Sorokin, V., Mace, B.: Response of linear parametric amplifiers with arbitrary direct and parametric excitations. *Mech. Res. Commun.* **109**, 103585 (2020)
47. Sorokin, V.: Longitudinal wave propagation in a one-dimensional quasi-periodic waveguide. *Proc. R. Soc. A Math. Phys. Eng. Sci.* **475**, 20190392 (2019)
48. Kim, C., Lee, C., Perkins, N.: Nonlinear vibration of sheet metal plates under interacting parametric and external excitation during manufacturing. *J. Vib. Acoust.* **127**, 36–43 (2005)
49. Zaghari, B., Rustighi, E., Ghandchi Tehrani, M.: Phase dependent nonlinear parametrically excited systems. *J. Vib. Control.* **25**, 497–505 (2018)
50. Mitropolskii, I., Dao, N.: *Applied asymptotic methods in nonlinear oscillations*. Springer, Dordrecht (2011)

**Publisher's Note** Springer Nature remains neutral with regard to jurisdictional claims in published maps and institutional affiliations.